Chapter 4

B^0 Meson Semileptonic Branching Fraction

4.1 Introduction

In this chapter, we partially reconstruct a $\bar{B}^0$ through the decay $\bar{B}^0 \to D^{*+}\ell^-\bar{\nu}_\ell$, $D^{*+} \to D^0\pi^+$ to tag neutral B events and reconstruct the B^0 meson inclusive leptonic spectrum.[1] By comparing the leptonic spectrum with an earlier CLEO analysis of the $\Upsilon(4S)$ inclusive leptonic spectrum, we are able to derive the charged and neutral B meson semileptonic branching fraction and the charged to neutral B lifetime ratio, τ_{B^+}/τ_{B^0}, assuming the isospin symmetry of B^- and $\bar{B}^0$ in semileptonic decay.

We will briefly review some previous analyses on B semileptonic decay, and discuss the motivation of B^0 tagging through the method of *partial reconstruction*. We outline the rest of this analysis as follows: The method of *partial reconstruction* will be discussed in section

[1] Charge conjugation is implied throughout this thesis.

4.4. We then lay out our event sample and tabulate our cuts in section 4.5 and 4.6. In section 4.7 we will focus on the inclusive lepton spectrum from B^0 semileptonic decay. The various systematic errors will be detailed in section 4.8. We then proceed to compare the different lepton spectra with an earlier CLEO analysis based on single lepton. The branching fraction, lifetime ratio and other interesting physics quantities will be calculated in section 4.10. Our summary and result will be laid out in section 4.11

4.2 B Semileptonic Branching Fraction

Over the past decade, there have been intensive research activities on semileptonic decays of B mesons. Despite various experimental and theoretical efforts, the measured semileptonic branching fraction of B meson decay is not in agreement with the theoretical prediction that the branching fraction of $Br(B \to X\ell\bar{\nu}_\ell)$ should be no less than 12.5% [57]. Most experimental values are found to be lower than that value.

The inclusive B semileptonic decay is denoted as $B \to X\ell\bar{\nu}_\ell$, where X means any hadrons, ℓ means electron or muon only. While the measurement of individual modes, for example $Br(B \to D^*\ell\bar{\nu}_\ell)$ and $Br(B \to D\ell\bar{\nu}_\ell)$ (**exclusive modes**) could probe the dynamics of B meson decay and measure the properties like q^2 distribution and value of V_{cb}, the **inclusive** analysis can give us the total inclusive branching fraction. Since the total B meson decay width is dominated by the width of B semileptonic decay and that of B hadronic decay, knowledge of the B semileptonic decay can effectively probe the hadronic portion of the B decay, which must be well measured in order to evaluate the CKM matrix elements.

There have been several measurements of inclusive B semileptonic branching fractions. The methods can be grouped as (1) single lepton analysis and (2) dilepton analysis for $\Upsilon(4S)$, and (3) lepton transverse momentum analysis in $Z \to b\bar{b}$ environment. The analyses

in $\sigma(Z \to b\bar{b})$ environment were performed by several LEP experiments (ALEPH, DELPHI, L3 and OPAL) at CERN. The $\Upsilon(4S)$ measurements were done by the CLEO and ARGUS collaborations.

4.2.1 Inclusive Lepton Analysis

In single lepton analysis [37, 38, 39, 40], all leptons are selected and used to construct the leptonic momentum spectrum. The spectrum consists of two main sources of leptons with very different shapes. Those shapes were calculated based on some theoretical models and are used to separate the primary leptons, which come directly from B meson decay, from secondary leptons, which are from the decay products of mesons such as D, ψ mesons and others. The total number of primary leptons estimated from the fit then will be normalized to the total number of $B\bar{B}$ events to give the semileptonic branching fraction averaged over the mixture of neutral and charged B in $\Upsilon(4S)$ event. Figure 4.1 shows the lepton spectrum of a previous CLEO B semileptonic decay measurement based on the single lepton method. There are two assumptions in this method: (1) there is no non-$B\bar{B}$ decay in $\Upsilon(4S)$ and (2) $\Upsilon(4S)$ resonance decays equally to charged and neutral B mesons, $f_{+-}/f_{00} = 1$, where f_{+-}, f_{00} are the fractions of charged and neutral B production in $\Upsilon(4S)$ decay, respectively. This analysis is rich in statistics and was the first accessible approach during the early period of detector running when limited data were available.

4.2.2 Dilepton Analysis

By looking at the inclusive lepton spectrum at Figure 4.1, we notice that for a lepton with momentum greater than 1.4 GeV/c, it is highly possible that this lepton is from the $B \to X\ell\nu$ decay. The charge of the lepton can also serve as the flavor tag of the b quark. If

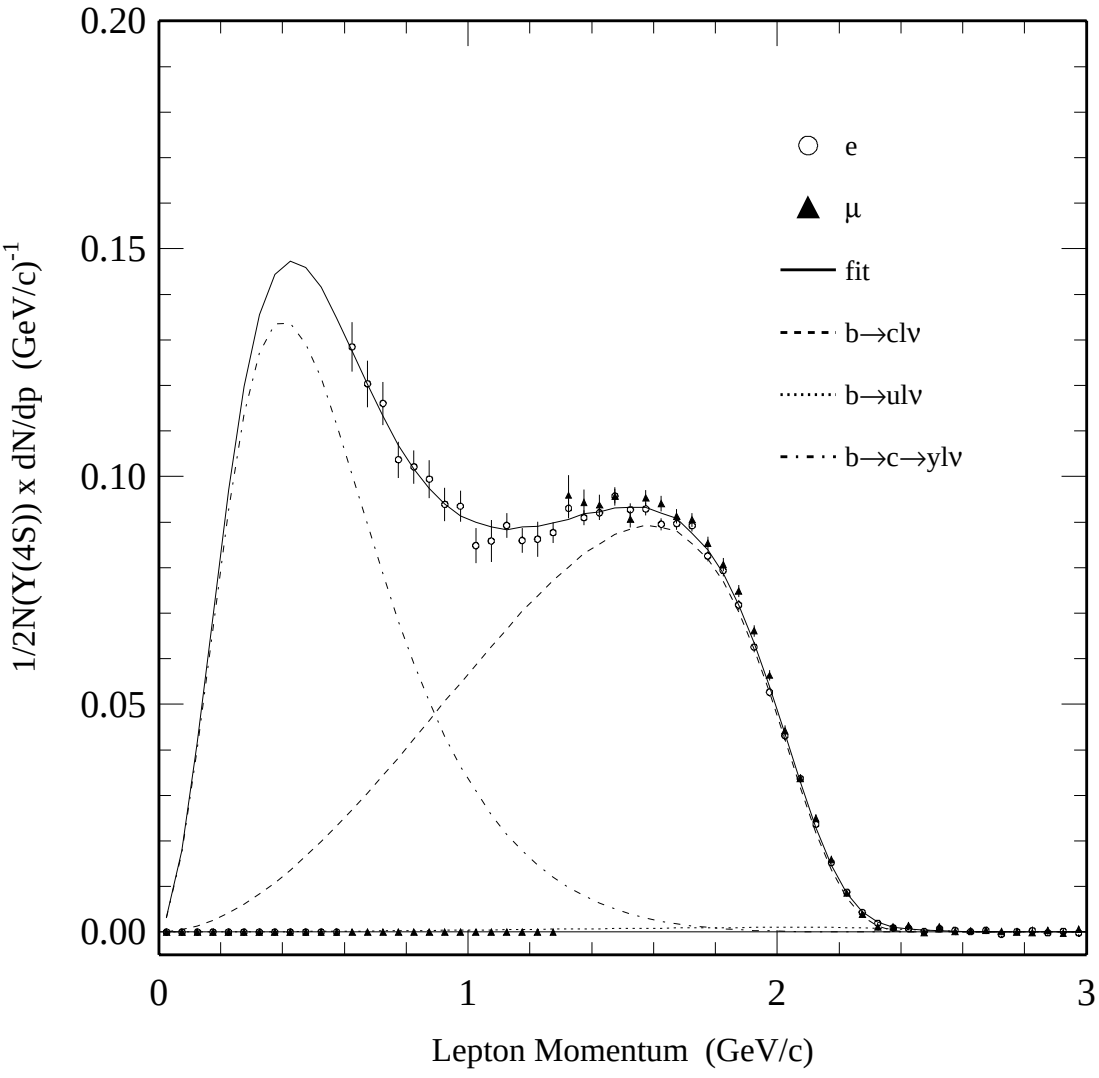

Figure 4.1: CLEO II B semileptonic decay lepton spectrum from single lepton measurement

the lepton carries the negative(positive) charge, it should come from the weak decay of $b(\bar{b})$ quark. This feature was used by the dilepton analysis.

In dilepton analysis, leptons with momentum greater than 1.4 GeV/c are used as a tag of the B meson, then a search is made for second leptons in the momentum range between 0.5 GeV/c to 2.5 GeV/c. This method then uses the correlation between charge and the angle of the secondary lepton that comes from the same B meson as the tag lepton. The angle θ between the two leptons, when the second lepton is from the same B meson as the tag, will mostly be $cos\theta < 0$, as the two leptons tend to decay back to back, with opposite charge. Second lepton from the the other B meson will not demonstrate such behavior as the distribution in $cos\theta$ is essentially flat. Through this correlation and the input of $B - \bar{B}$ mixing parameter χ_d, a model independent inclusive primary and secondary lepton spectrum averaged over neutral and charged B mesons is obtained [44, 45]. The primary and secondary lepton spectrum from this di-lepton analysis can be seen in Fig 4.2.

This method eliminates the assumption that $\mathrm{B}(\Upsilon(4S) \rightarrow B\bar{B}) = 100\%$. It also does not rely on theoretical models to predict the primary and secondary leptons in the lepton momentum spectrum. But this analysis can not differentiate the neutral from charged B meson.

4.2.3 Lepton Transverse Momentum Measurement

For experiments at the energy of Z boson production, the B mesons are produced incoherently. B mesons created here are also boosted to a larger momentum, thus making higher momentum leptons from B meson primary decay. Primary leptons from B meson decay can usually be characterized as having large momentum transverse to the jet axis. By fitting th distribution of both the transverse momentum, P_t, and P from the theoretical models, a measurement on B semileptonic branching fraction is made, see the LEP analysis [41, 42, 43].

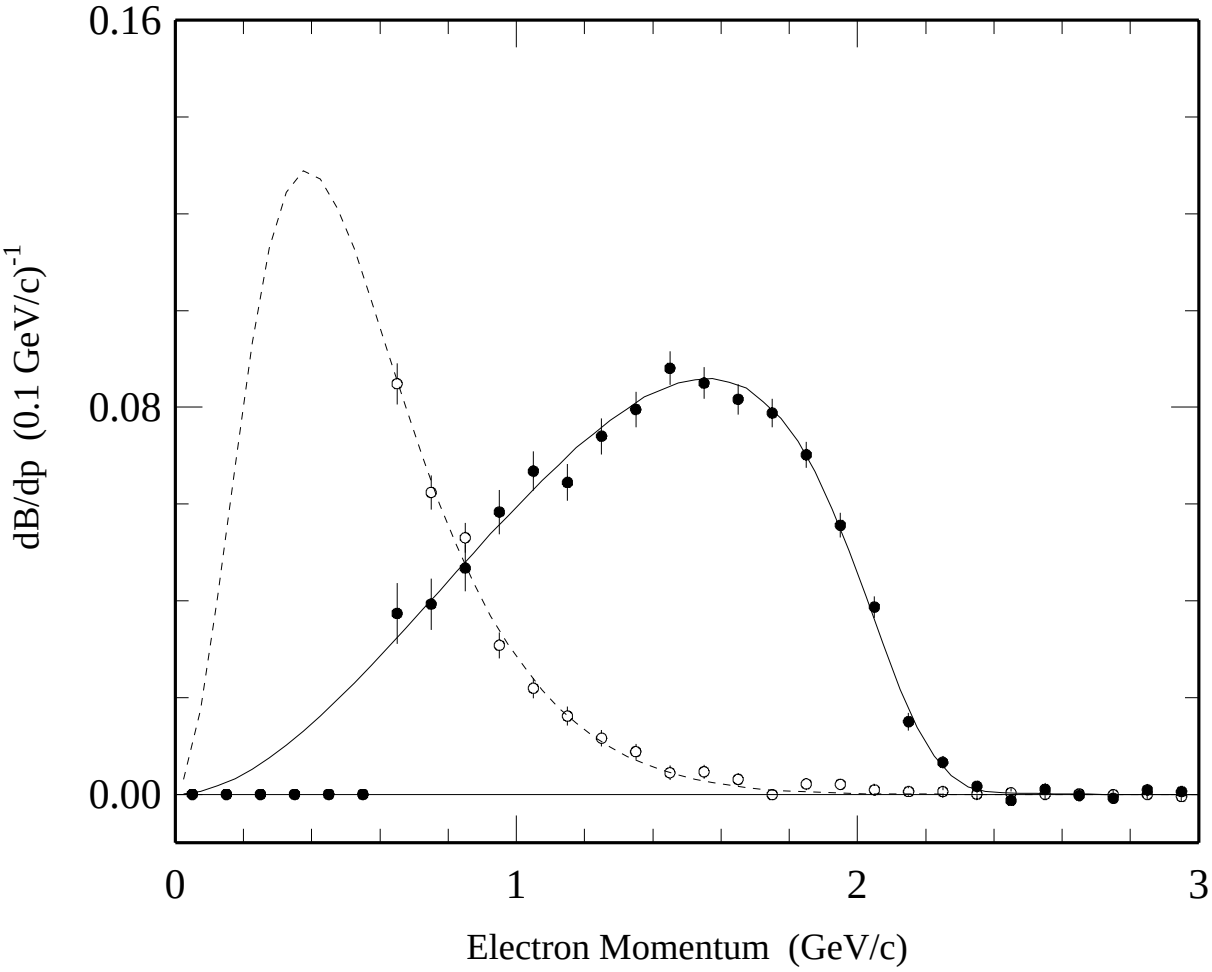

Figure 4.2: CLEO II B semileptonic decay lepton spectrum from dilepton measurement

4.3 Motivation of Partial Reconstruction

Both the single and di-lepton analyses can not differentiate $\bar{B}^0$ from B^-. Since the averaged B semileptonic branching fraction is less than theory has predicted, the natural step is to measure the semileptonic branching fraction of $\bar{B}^0$ and B^- separately. Tagging the charge of the B meson can remove such uncertainty. The first method that comes to mind is to explicitly reconstruct a $\bar{B}^0(B^-)$ meson. For example, using the decay chain:

$$\begin{aligned} \bar{B}^0 &\rightarrow D^{*+}\ell^-\bar{\nu}_\ell \\ & \quad D^{*+} \rightarrow D^0\pi^+ \\ & \quad\quad D^0 \rightarrow K^-\pi^+ \end{aligned}$$

Although the ambiguity of neutral/charged B meson has been eliminated, the statistical power suffers because $Br(D^0 \rightarrow K^-\pi^+)$ is only 3.8%. Including $D^0 \rightarrow K^-\pi^+\pi^0$, a mode with branching fraction about 13.9%, does not increase the statistical power much, because we have a large amount of $\pi^0 \rightarrow \gamma\gamma$ combinatorial background. We would like to gain a clean signal with good statistical power and to reduce the systematic uncertainty as much as possible.

With this in mind, the method of *Partial Reconstruction* was developed. This method takes advantage of the character of $\Upsilon(4S)$ decay and the strong correlation between the π^+ from D^{*+} decay, without explicitly reconstructing the D^0. If we compare this with the B^0 tagging through exclusive D^0 reconstruction, we can immediately know that by not reconstructing D^0, the statistics increase by a factor of 25.

This method was first suggested by CLEO in 1983, then employed by ARGUS and CLEO as a tag of $\bar{B}^0$ meson [47, 50, 49]. We will explain the method of *partial reconstruction* later. It also has been explained in detail elsewhere [48].

4.4 Analysis Overview

The strategy of this analysis is to use the **partial reconstruction** method to tag a neutral $\bar{B}^0/B^0$. For each tagged event, we then look for additional charged leptons from semileptonic $B^0/\bar{B}^0$ meson decay, to reconstruct the lepton spectrum of the opposing B. We extract the portion of primary leptons in this reconstructed additional lepton spectrum. The ratio of the number of *additional primary leptons* to the total number of tags will lead us to the B^0 semileptonic branching fraction. It can be visualized as follows:

$$X\ell^{\pm}_{\mathbf{add}}\bar{\nu}_\ell \leftarrow \boxed{B^0/\bar{B}^0, \bar{B}^0} \rightarrow D^{*+}\ell^{-}_{\mathbf{tag}}\bar{\nu}_\ell$$
$$D^{*+} \rightarrow D^0\pi^{+}_{\mathbf{tag}}$$

We obtain N_{tag}, the number of tags, $(\ell^{\pm}_{tag}, \pi^{\mp}_{tag})$, and extract N_ℓ, the number of additional primary leptons in the tagged event, $(\ell_{add}, [\ell^{\pm}_{tag}, \pi^{\mp}_{tag}])$. The ratio of those two number: N_ℓ/N_{tag} is b_{tag}, the semileptonic branching ratio in an event sample highly enriched in B^0. The semileptonic branching fraction measured in inclusive analysis mentioned earlier is obtained in a sample that has a roughly equal mixture of B^0 and B^-. By comparing these two numbers, one can obtain the neutral and charged B semileptonic branching fraction , b_+ and b_0, respectively. Using isospin symmetry in $\bar{B}^0$ and B^- semileptonic decay, we can obtain the lifetime ratio of charged to neutral B, τ_+/τ_0.

For reasons mentioned earlier in the discussion on di-lepton analysis, we require the tag lepton to be within the momentum range 1.4-2.4 GeV/c.

The tagged pion is moving slowly. We require the momentum of the tagged pions to be lower than 190 MeV/c. The tagged lepton and pion pair should carry opposite charges for the signal decay. This opposite charge lepton-pion pair is denoted as the "right sign" combination.

For additional leptons, we require the momentum to be in the range 0.5 GeV/c - 2.5 GeV/c and 1.5 - 2.5 GeV/c for electrons and muons, respectively. We reconstruct the additional lepton spectrum for electrons and muons separately.

4.5 Data and Event Cuts

We use the CLEO II [32] (4s2 - 4sA) data set which has an integrated luminosity of 2.38 fb^{-1} taken at the $\Upsilon(4S)$ resonance, and 1.13 fb^{-1} taken at off resonance, which is 60 Mev below the $\Upsilon(4S)$. All events considered here are required to pass our standard hadronic criteria, which require at least 3 well-fitted charged tracks, a measured energy at least 0.15 times the center of mass energy and an event vertex consistent with the known interaction point (KLASGL = 10). We select hadronic events with at least 5 charged tracks (NTRKCD $\geq$ 5). To suppress continuum background, we require the ratio of Fox-Wolfram [86] moments to be less than 0.4 (R2GL $<$ 0.4).

Leptons in the tag are required to have momentum between 1.4 GeV/c and 2.5 GeV/c. Electrons are further required to have R2ELEC $\geq$ 3.0, and muons are required to have MUQUAL = 0 and DPTHMU $\geq$ 5. The tagged lepton candidates must come from the fiducial region $|CZCD| < 0.79$ and satisfy the standard CLEO-II tracking cuts. For additional leptons, the momentum must be within 0.5 GeV/c to 2.5 GeV/c for electrons, and 1.5-2.5 GeV/c for muon candidates. All the cuts for leptons are listed as follows:

For tag lepton,

- $KINCD = 0$ (good fitted track)
- $NHITPT + NHITVD > 0$ (must have at least one PT or VD hit)
- $RHITDR > 0.4$ (40% of DR penetration)

- at least any two of the following:
  - $|DBCD| < 5$ mm
  - $|ZOCD| < 5$ cm (within 5 centimeter in z of interaction point)
  - $RESICD < 1$ mm (tracking quality fit cut)
- 1.4 GeV/c $< P_\ell <$ 2.5 GeV/c
- for electron
  - R2ELEC ≥ 3.0
- for muon
  - MUQUAL $= 0$
  - DPTHMU ≥ 5.0
  - $|CZCD| \leq 0.79$

Pions in the tag must have a charge opposite to that of the tag lepton and pass the following cuts:

- $P_\pi \leq 0.190$ GeV/c
- $KINCD = 0$ (good track)
- $|SGPIDI| < 2.0$ (within 2 σ of π ID from dE/dX)
- $|DBCD| < 5$ mm
- $|ZOCD| < 5$ cm.

For second lepton, same as for tagged lepton except:

- for second lepton as electron
  - 0.5 GeV/c $< P_\ell <$ 2.5 GeV/c
  - $|CZCD| < 0.7071$
- for second lepton as muon
  - 1.5 GeV/c $< P_\ell <$ 2.5 GeV/c
  - $|CZCD| < 0.61$

4.5.1 $\pi^{\pm}$ Identification

The kinematic cut on the pion is a little bit tighter than the maximum momentum allowed for pions from $\bar{B^0} \to D^{*+}\ell\bar{\nu}_\ell, D^{*+} \to D^0\pi^+$ decay, which is about 225 MeV/c. The particle identification for pion relies on the dE/dX identification using information from the drift chamber. It works very well for such a low momentum pion.

Pion momentum smaller than 60 MeV/c can not be detected because the reconstruction efficiency for a charged track that slow is very small. Small momentum charged tracks tend to leave few hits in the drift chamber, making it hard to reconstruct the tracks. CLEO has studied the pion tracking reconstruction efficiency and has simulated the data with Monte Carlo [63].

As we have discussed in the previous chapter, the existence of a strong magnetic field will make the low momentum charged tracks highly curved, meaning that track could have multiple hits in each of several layers. Since the tracking reconstruction takes only one hit per layer, multiple hits in one layer belonging to a single track could be used to reconstruct as two or more tracks. This creates "ghost tracks", where two or more tracks are reconstructed from a single particle. We use the TRKMAN processor [35] to eliminate ghost tracks. TRKMAN

considered the two tracks as "ghost pair" when there are two tracks in the event with very similar curvature and ϕ value, but there are very few layers where both tracks have a hit. The track of the pair which has fewer stereo and cathode hits is rejected, taking the track with better z position measurement as the real track.

Monte Carlo study shows CLEO tracking reconstruction routine, DUET processor, makes about 3.5 mistakes per $B\bar{B}$ event. The TRKMAN/TMNG reduced the number of mistakes by a factor of two [35].

4.5.2 Lepton Identification

Fake Lepton

Some hadronic tracks will be identified as leptons when they leave traces in the Crystal Calorimeter and/or in the Muon Chamber. The "Fake Lepton" candidates need to be accounted for and subtracted as background. CLEO has studied this fake lepton effect and come up with a fake rate as a function of momentum for different hadron species [46].

Fake rate is the probability of misidentifying a hadron as an electron or muon and is momentum dependent. The probabilities of pion, proton and kaon to pass the lepton identification are different from each other. CLEO [46] has studied the fake lepton probability of K, p, π in $\Upsilon(4S)$ respectively. CLEO selects charged pions from $K_s \to \pi^+\pi^-$, protons from $\Lambda \to p\pi$, kaons from $D^* \to D^0\pi$, $D^0 \to K\pi$. While we have many pions and an adequate number of protons in our data sample, the amount of $\Upsilon(4S)$ events was not enough to produce kaons through $D^0 \to K\pi$. Due to the lack of statistics for the $\Upsilon(4S)$, especially for the kaon sample, we used the fake rates obtained from $\Upsilon(1S)$ sample [46] to produce the fake rate with the fine momentum distribution this analysis required.

Unlike $\Upsilon(4S)$, hadronic decays in $\Upsilon(1S)$ are not expected to produce leptons. Therefore

fake rates can be calculated simply by counting $\Upsilon(1S)$ tracks which passed the lepton identification packages. The only sources of real leptons are from the decay $\Upsilon(1S) \to \gamma^* \to q\bar{q}$ which has the same physics as in the continuum. This source of real leptons were removed by appropriately scaling the OFF resonance data sample and subtracting from $\Upsilon(1S)$.

There is good agreement between the two measurements and we have used the difference as an estimate of systematic error in the fake lepton correction. Figure 4.3 shows the electron and muon fake rate study of $\Upsilon(1S)$ and $\Upsilon(4S)$.

In this analysis, we use hadronic tracks that failed the lepton identification criteria and sort according to their momentum, then multiply the fake rate in that particular momentum range to obtain the number of fake leptons in that momentum bin. These fake leptons will be subtracted from our lepton samples.

Lepton Identification Efficiency

Muon Identification

MUTR [71] processor is used for muon identification information. Each track is extrapolated into muon chamber and matched to muon hits on the basis of their separation. A track must have two hits in a particular superlayer to be considered a muon candidate. If the muon has hits at a deeper layer but none at a layer of shallower depth, the track quality MUQUAL is registered as non-zero to flag this muon track candidate as not good. The variable DPTHMU marks the depth of the outermost layer with a hit. The larger the muon momentum is, the deeper the muon hits. For the case of DPTHMU > 3.0, the muon momentum is greater than 1.4 GeV/c.

The efficiency for muon identification is determined by the chamber efficiencies and the

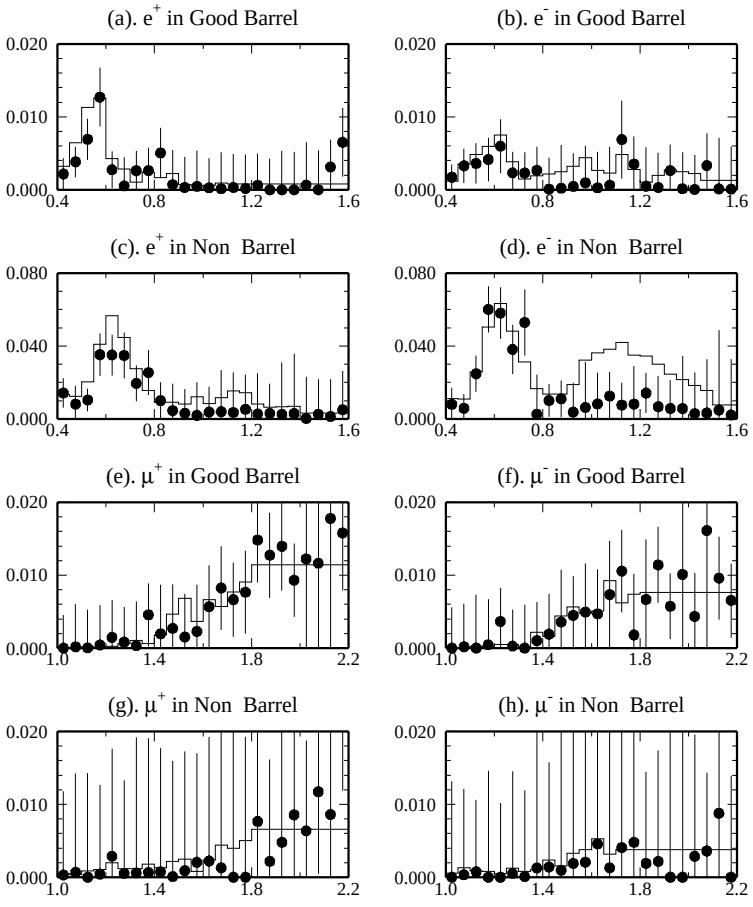

Figure 4.3: electron and muon fake rate: $\Upsilon(1S)$ (histogram) overlaid by $\Upsilon(4S)$(dot). Good agreement shown in good barrel region, where the electron and muon candidates are taken. (Courtesy of Dr. Roy Wang Ph.D thesis)

momentum dependent energy loss experienced by muons in the materials in front of each muon chamber. Monte Carlo simulates the chamber efficiency for each layer to within $\pm 1\%$ error [46]. The energy loss in the material is understood at a level of 10 MeV [73].

Electron Identification

CLEO electron identification package CEID combines the available information from several sources to form a probability variable, R2ELEC, for electron ID. Those sources include: (E/P), the ratio of the energy measured in the electromagnetic calorimeter to the momentum of the track, the dE/dX, the track-crystal shower matching, the shower shape in the crystals and information from TF. The probability variable, R2ELEC, is written as:

$$R2ELEC = \sum_i ln(\frac{P_e}{P_{\neq e}})_i \tag{4.1}$$

Here P_e and $P_{\neq e}$ are the probabilities of a charged track being identified as an electron or hadron based on that source i. P_e were determined by embedding the bhabha electrons into hadronic events. $P_{\neq e}$ is determined by data taking at $\Upsilon(1S)$ events, where very few electrons are produced.

CLEO has studied the electron identification efficiency [46]. The tracks from radiative Bhabha events in data are embedded into hadronic events from data to assess electron identification in $B\bar{B}$ events. The efficiency is found generally to be above 90%. The uncertainty in electron efficiency has been estimated to be about 2%. The muon identification efficiency estimated from Monte Carlo and electron efficiency measured from embedding study is shown in Fig 4.4.

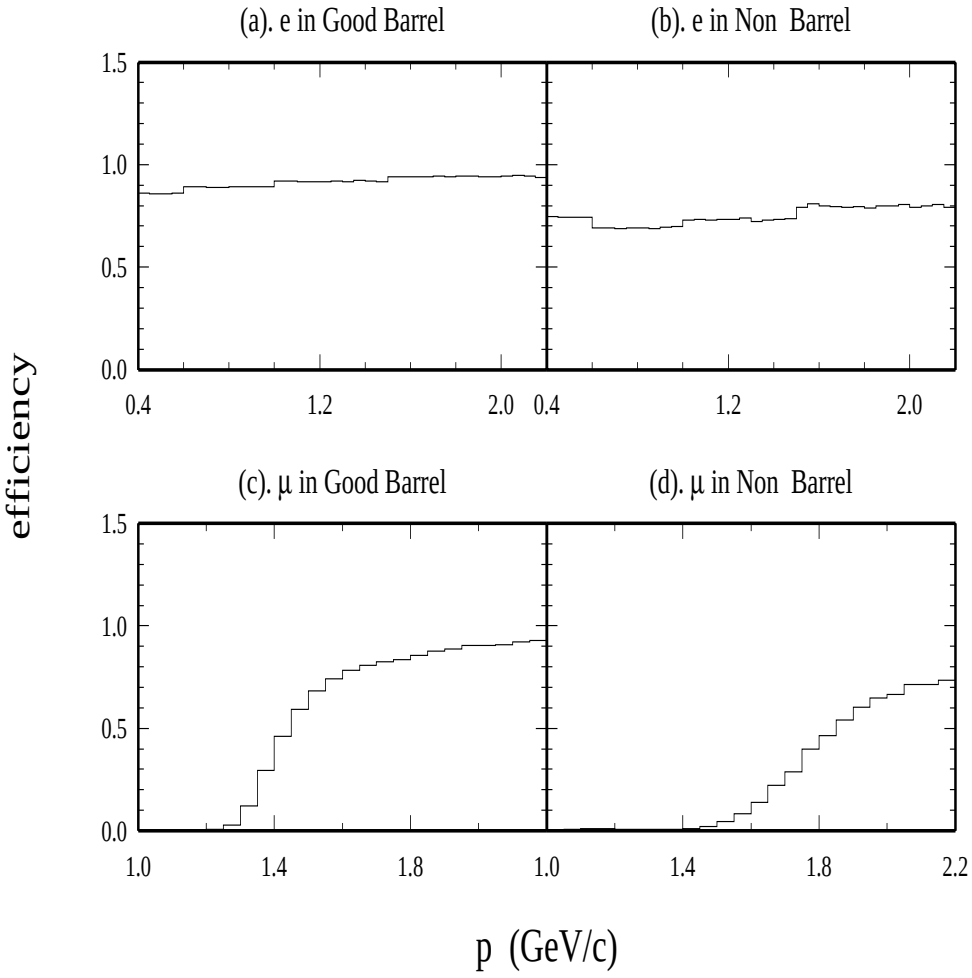

Figure 4.4: The lepton identification efficiency. Electron ID efficiency obtained from track embedding study and muon ID efficiency from Monte Carlo

4.6 Partial Reconstruction of B^0

In this section, we will describe the technique of *partial reconstruction* in detail.

B's produced at $\Upsilon(4S)$ are tagged through partial reconstruction of the semileptonic decay $B \to D^{*+}\ell^-\bar{\nu}_\ell, D^{*+} \to D^0\pi^+$, without explicitly reconstructing the D^0. In brief, we can use the soft pion from D^{*+} decay to approximate the four momentum of D^{*+} by taking advantage of the extremely low phase space available in $D^{*+} \to D^0\pi^+$. Combining with the detected lepton, we can calculate the mass square of the neutrino, which is also called "missing mass square" in other literature and we will use this term from now on. For leptons and pions coming from the signal decay, the calculated missing mass square value should be close to zero.

The four momentum of D^{*+} can be approximated by the pion from $D^{*+} \to D^0\pi^+$ as:

$$E_{D^*} \simeq \frac{E_\pi}{E_\pi^{CM}} M_{D^*} \equiv \widetilde{E}_{D^*}, \mathbf{p}_{D^*} \simeq \frac{\mathbf{p}_\pi \times \sqrt{\widetilde{E}_{D^*}^2 - M_{D^*}^2}}{|p_\pi|} \equiv \widetilde{\mathbf{p}}_{D^*} \tag{4.2}$$

where E_π is the the π^+ energy in the lab frame, $E_{\pi^+}^{CM} \approx 145$ MeV is the energy of the π^+ in the D^{*+} rest frame, and M_{D^*} is the mass of the D^{*+}. Because the B momentum in $\Upsilon(4S)$ is very small, about 300 Mev/c, we can approximate $\mathbf{p_B} \simeq 0$. The square of the neutrino mass (*missing mass square*) is:

$$\widetilde{M_\nu^2} \equiv (E_{\text{beam}} - \widetilde{E}_{D^*} - E_\ell)^2 - (\widetilde{\mathbf{p}}_{D^*} + \mathbf{p}_\ell)^2. \tag{4.3}$$

There are several approximations made in this method. The study on such approximations has been documented in great detail in [48]. The discussions below follows directly from that pioneer study.

The complete expression of M_ν^2 is:

$$\begin{aligned} M_\nu^2 &= E_\nu^2 - P_\nu^2 = (E_{\rm beam} - E_l - E_{D^*})^2 - |\vec{P}_B - \vec{P}_l - \vec{P}_{D^*}|^2 \\ &= (E_{\rm beam} - E_l - E_{D^*})^2 - |\vec{P}_l + \vec{P}_{D^*}|^2 - P_B^2 + 2\vec{P}_B \cdot (\vec{P}_l + \vec{P}_{D^*}). \end{aligned} \tag{4.4}$$

In $\Upsilon(4S)$ resonance, the B meson is moving with approximately $|P_B| = 300$ MeV/c and we do not know its direction. The last two terms associated with B meson momentum in the lab frame on average contribute to about 0.002 GeV^2. Approximating $|P_B| = 0$ will widen the resolution of $\widetilde{M_\nu^2}$ to 0.4 GeV^2 and not significantly move the mean of $\widetilde{M_\nu^2}$ from zero.

Secondly, the energy of D^{*+} is approximated by the slow pion. The energy of charged pion in the lab frame can be calculated as follow:

$$E_\pi = \gamma(E_\pi^{CM} + \beta P_\pi^{CM} cos\theta) \tag{4.5}$$

where the $cos\theta$ is the cosine angle between pion in the D^{*+} frame and the direction of D^{*+} seen in the lab. The γ and β are the lorentz transformation factor to boost π from the center of mass frame of D^* to the lab frame. The term proportional to $cos\theta$ is canceled by taking the average. γ can then be approximated as:

$$\gamma \simeq \frac{E_\pi}{E_\pi^{CM}} \equiv \hat{\gamma} \tag{4.6}$$

This $\hat{\gamma}$ enables us to calculate the average energy of D^{*+}:

$$E_{D^*} \simeq \hat{\gamma} M_{D^*} = \frac{E_\pi}{E_\pi^{CM}} M_{D^*} \equiv \widetilde{E_{D^*}} \tag{4.7}$$

The resolution of γ, then D^{*+} energy, depends on the polarization of D^{*+}. It is estimated to be about 8% [48]. This approximation is better for D^{*+} of helicity $= \pm 1$ than for D^{*+} of helicity $= 0$ since π^+ are preferentially emitted towards $cos\theta = 0$ and consequently experienced the same boost as the D^{*+}. The Fig 4.5 shows the ratio $(\hat{\gamma} - \gamma)/\gamma \equiv \delta\gamma/\gamma$ for unpolarized and polarized D^*.

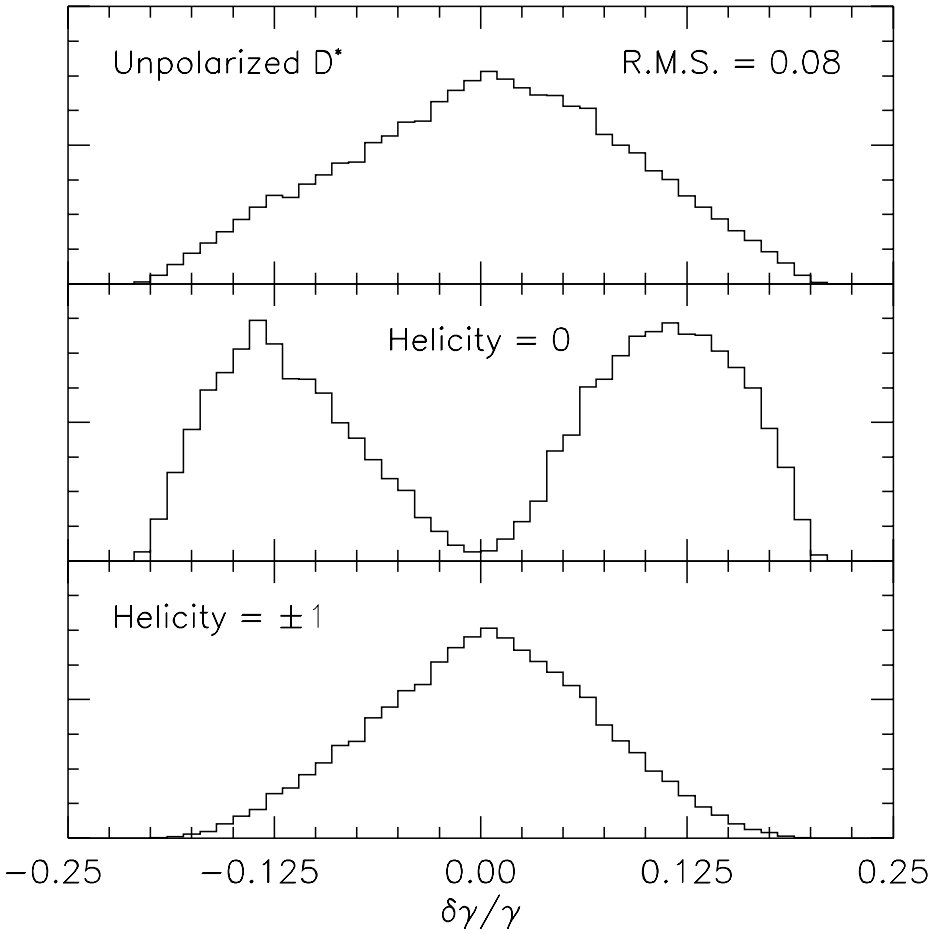

Figure 4.5: Error on Gamma approximation. Courtesy of Mike Sauliner Ph.D thesis [48].

The third approximation is to assume that the direction of the soft π is the same as that of the D^{*+} seen in the lab. It is estimated from Monte Carlo [48] that the direction approximation also depends on the polarization of D^{*+} meson, but works better for helicity 0 D^{*+} meson than for D^{*+} meson with helicity 1. This is just opposite to the energy approximation we mentioned previously.

The combination of the the last two approximations give us about 600 Mev/c uncertainty in D^{*+} momentum. Comparing this with the error of momentum approximation in B meson, $P_B \simeq 300 MeV/c$, we expect the width of $\widetilde{M_\nu^2}$ resolution in the *partial reconstruction* won't be much wider than twice 0.4 GeV^2. The Monte Carlo simulation did find the error to be $\simeq 0.9\ GeV^2$ as can be seen in Fig 4.6 [48].

4.7 B^0 Tag from Partial Reconstruction

There are two major backgrounds to be subtracted in our tag sample, the continuum and the combinatorial background. The continuum background occurs when the lepton and pion tracks do not come from $\Upsilon(4S)$ event, but from $e^+e^- \to q\bar{q}$, where q means u, d, s and c quark. The combinatoric background from $B\bar{B}$ events are the random combination of the oppositely charged lepton-pion pairs which pass our kinematic cuts.

4.7.1 Continuum Background Estimation

To estimate the continuum background, we analyze events taken at *Off* resonance energy. The $\widetilde{M_\nu^2}$ of the oppositely charged lepton-pion pair was calculated from events 60 MeV below the $\Upsilon(4S)$ resonance. The resulting histogram was scaled for the luminosity and energy difference to obtain the continuum events in the $\Upsilon(4S)$ data. We then subtract this scaled

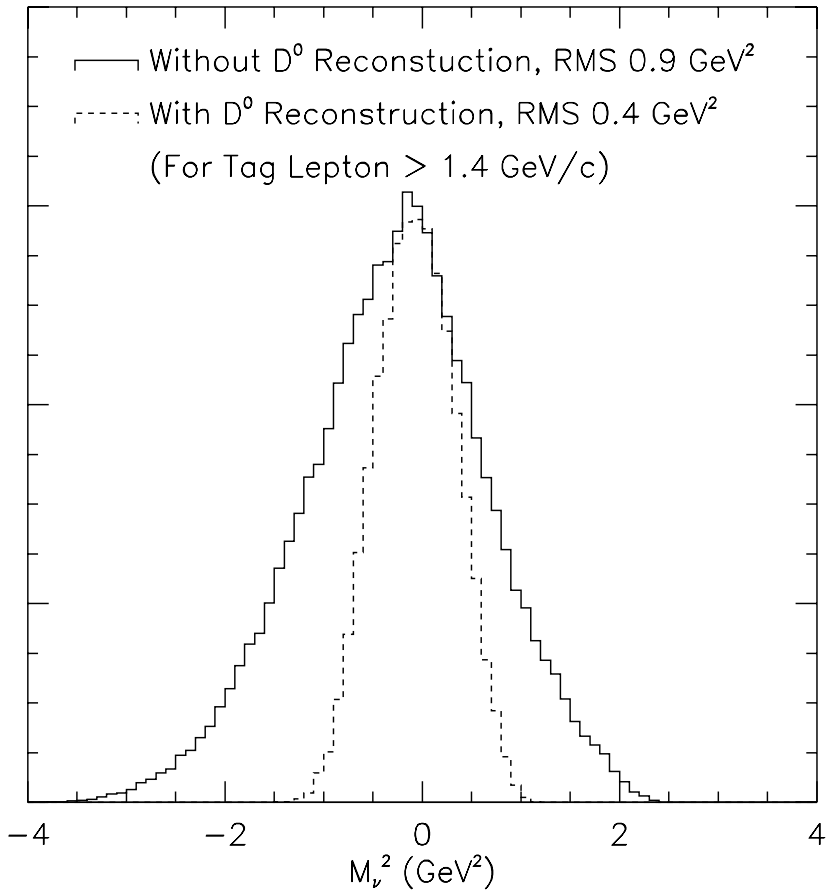

Figure 4.6: The missing square signal for tag lepton $P_\ell > 1.4$ GeV/c with and without D^0 reconstruction, from [48].

continuum from data. The scaling factor is calculated as follows:

$$Scaling\ \ Factor = \frac{L_{on}}{L_{off}} \frac{E^2_{beam}(off)}{E^2_{beam}(on)} = 2.11 \tag{4.8}$$

The L_{on} and $E_{beam}(on)$ correspond to the luminosity and energy of the beam at the $\Upsilon(4S)$. and L_{off}, $E_{beam}(off)$ correspond to the values in off resonance data.

4.7.2 Combinatoric Background Estimation

We use CLEO generic $B\bar{B}$ Monte Carlo to simulate this combinatoric background. The scaling factor for Monte Carlo is obtained by matching the entries of Monte Carlo to Data in the **side-band region**, $-25 \leq \widetilde{M^2_\nu} \leq$ -4 GeV^2. Only the entries in the signal region, $-2 \leq \widetilde{M^2_\nu} \leq 5$ GeV^2, after subtracting from combinatoric background will be collected to account as the tag, N_{tag}. In Fig 4.7 is the $\widetilde{M^2_\nu}$ of data, overlayed by continuum and Monte Carlo estimated combinatoric background. The net signal after the continuum and combinatoric background subtraction can be seen in Fig 4.8.

To know if our Monte Carlo simulates the data correctly, we take the wrong sign lepton-pion combination, where the tag leptons and pions have the same charge, and repeat the same procedure as we did for the right sign sample, $(\ell^{\pm}_{tag}, \pi^{\mp}_{tag})$. In Fig 4.9 we can see the result of wrong sign sample $\widetilde{M^2_\nu}$ in the signal region is consistent with being zero. This confirms our Monte Carlo has simulated the combinatoric background well in our data.

It is important not to use the wrong sign combination in the data as the combinatoric background in our right sign tag. The wrong sign and right sign combinatoric background have different composition ratios of correlated/uncorrelated background, where lepton and pion are from the same B/different B. Because the correlated and uncorrelated background have different missing mass square shapes, this results in different $\widetilde{M^2_\nu}$ shapes for right sign

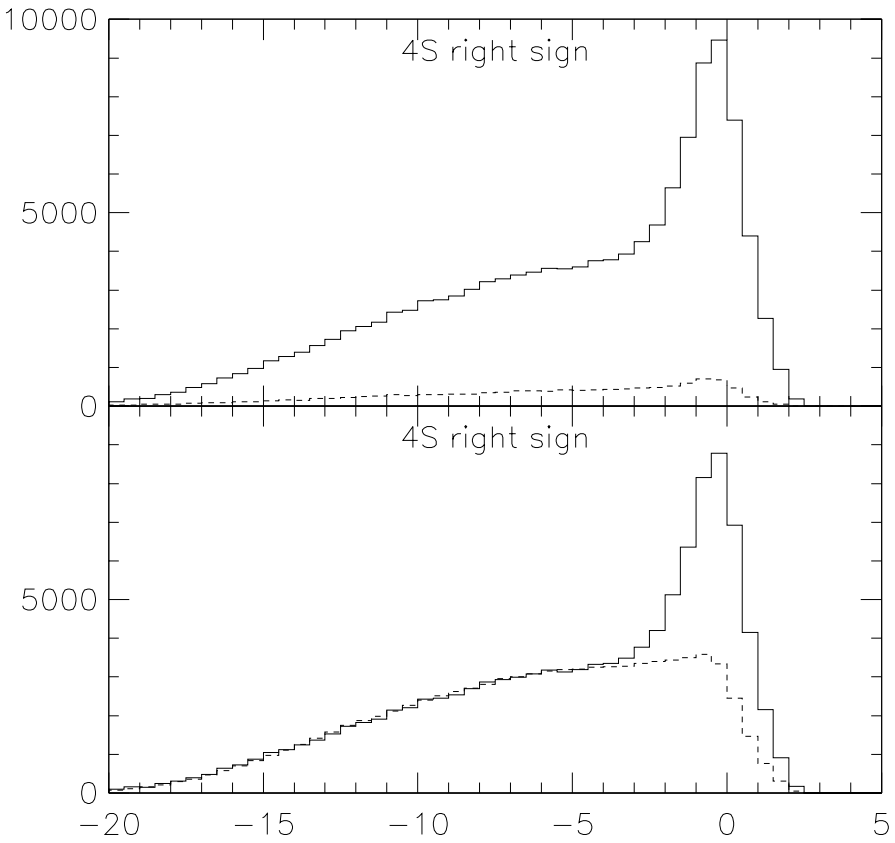

Figure 4.7: Right sign missing mass square overlayed by continuum (dash line) for above. The bottom plot is the continuum subtracted plot overlaid with random background (dash line). Only the entries between $-2 \leq \widetilde{M_\nu^2} \leq 5\ Gev^2$ region is counted as signal tag.

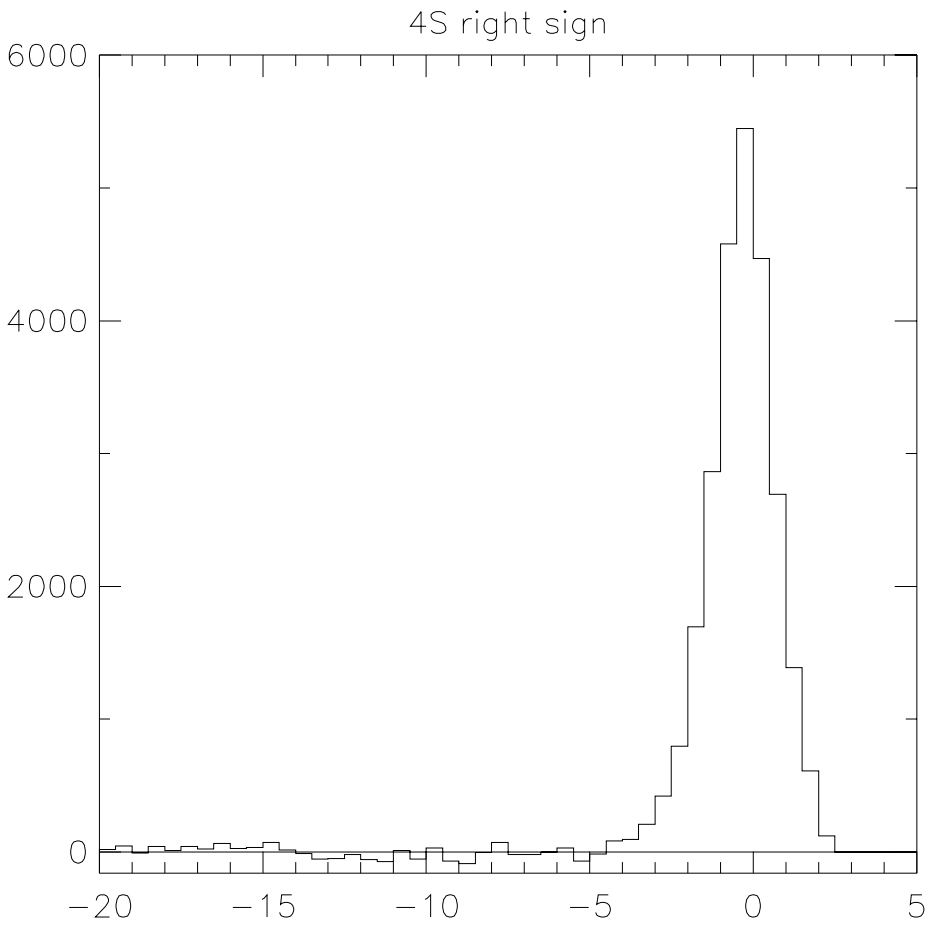

Figure 4.8: The missing mass square plot for tag signal after continuum and combinatoric background subtraction. We see a nice peak in our signal region ($-2 \leq \widetilde{M_\nu^2} \leq 5\ Gev^2$) and there is no tail.

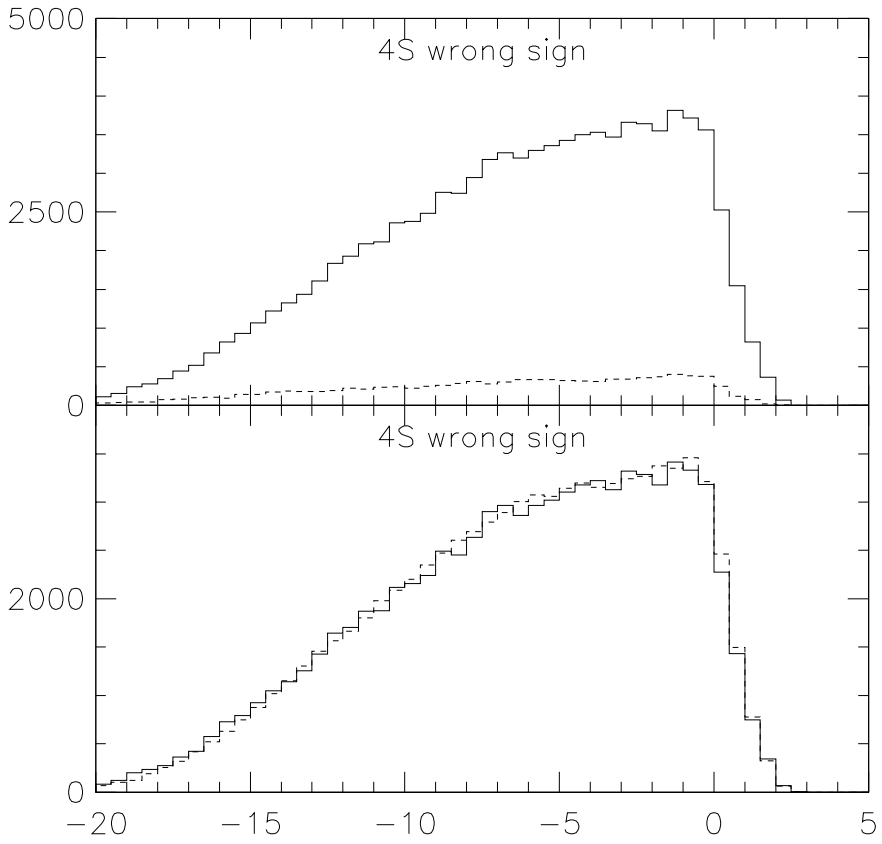

Figure 4.9: wrong sign missing mass square plot. As the case for right sign, the dashed line stands for continuum at the top, and the combinatoric background at the bottom. We see the Monte Carlo simulates the wrong sign background very well

Table 4.1: Number of Tags

Source	right sign	wrong sign
data(signal region)	46118.0 ± 214.8	19970.0 ± 141.3
continuum(signal region)	7043.9 ± 121.1	4164.7 ± 93.15
data-continuum(signal region)	39074 ± 246.58	15805 ± 169.28
data-continuum(side band)	47265.0 ± 306.6	45043.0 ± 293.4
MC background(side band)	211341 ± 459.7	210108 ± 458.4
MC background(signal)	178373 ± 422.35	78379 ± 279.96
scaling factor	0.2236	0.2144
MC scaled bg(signal region)	16194.0 ± 94.5	16803.0 ± 58.7
yield	22880 ± 283.0	-277.27 ± 179.2

and wrong sign background.

For tags in the signal region, we have gathered 46118.0 ± 214.8 for events taken at $\Upsilon(4S)$, 7043.9 ± 121.1 for events at continuum and 16194.0 ± 94.5 for events estimated as combinatoric background. The overall number of tagged lepton-pion pairs, $N(\ell^{\mp}_{tag}, \pi^{\pm}_{tag})$ after this procedure is: $N_{tag} = 22880 \pm 283(stat)$ We tabulate the numbers related with these tags in Table 4.1.

4.8 Additional Lepton Spectra Reconstruction

After a tag lepton-pion pair has been found, a search for additional leptons in the same event is performed. The $\widetilde{M^2_\nu}$ distribution is calculated as we did for the tag, except we now sort it in 100 MeV/c bins in terms of the additional lepton's momentum. We also separate the second lepton according to its particle species. The additional leptons include all leptons except the one being counted as tag in the event.

In each bin of $\widetilde{M^2_\nu}$, we subtract the contributions from continuum, additional leptons that are fake and combinatoric background. After those subtractions, the remaining entries in the signal region will be used to construct our second lepton momentum spectrum.

This spectrum will be corrected for lepton identification and reconstruction efficiency. Then the additional leptons from $B \to J/\psi \to \ell^+\ell^-$ decay are subtracted to obtain the lepton momentum spectrum for fitting.

This reconstructed additional lepton spectrum contains leptons from primary leptons, $b \to \ell$, secondary leptons, $b \to c \to \ell$ and leptons from "other sources" like D_s, τ, Λ_c, photon conversion, and π^0 dalitz decay. The leptons from "other sources" will be denoted as "other leptons". The contribution of these "other leptons" are very small compared with primary and secondary leptons. Their contaminations will be studied in the systematic error section.

4.8.1 Continuum, Fake Lepton and Random Background

The continuum background was estimated by taking events at off resonance data and scaling to account for the energy and luminosity difference in $\Upsilon(4S)$. For the fake leptons estimation, we first replace the additional leptons with any charged hadronic tracks that pass all the additional lepton cuts except the lepton ID. We then subtract the hadron-tag sample that are from the continuum. The result will be multiplied by the corresponding fake rate in that charged hadronic track momentum to obtain the number of fake leptons at that particular momentum bin.

After the continuum and fake additional lepton entries have been subtracted, we then subtract random background in the same way as we did for the tag. The entries collected at signal region ($-2 \leq \widetilde{M_\nu^2} \leq 5$ GeV/c^2) in missing mass square distribution for each bin will be the entries of the additional leptons in that particular momentum bin to construct the inclusive lepton momentum spectrum. Plots in Fig 4.10, Fig 4.11, Fig 4.12 are the bin-by-bin $\widetilde{M_\nu^2}$ distribution of tag with second electrons from 0.5-2.5 GeV/c and muons at momentum 1.5-2.5 GeV/c each, respectively. Their respective entries bin-by-bin are listed at Table 4.2

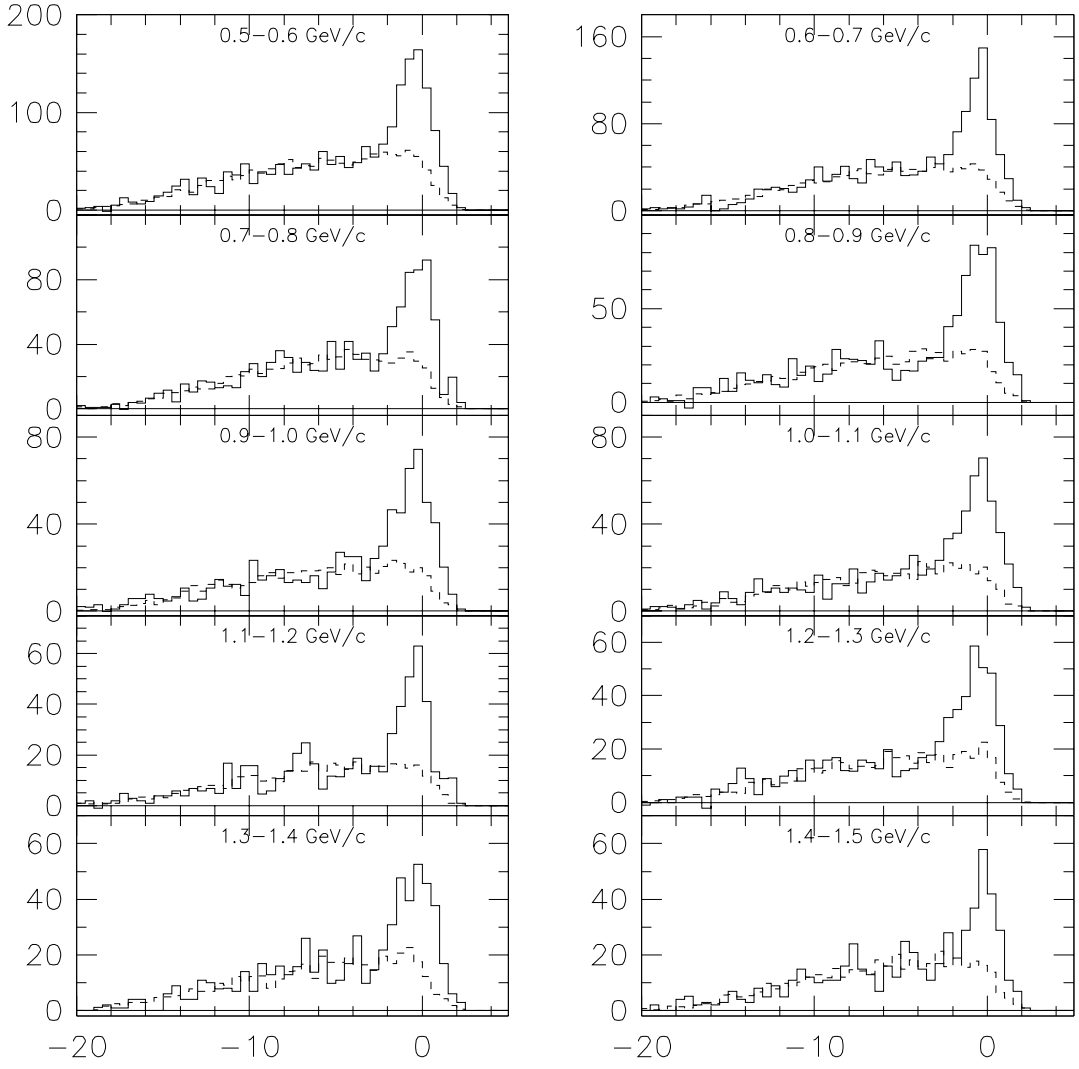

Figure 4.10: $\tilde{M}_\nu^2$ bin-by-bin for second lepton (electron) momentum between 0.5-1.5 GeV/c

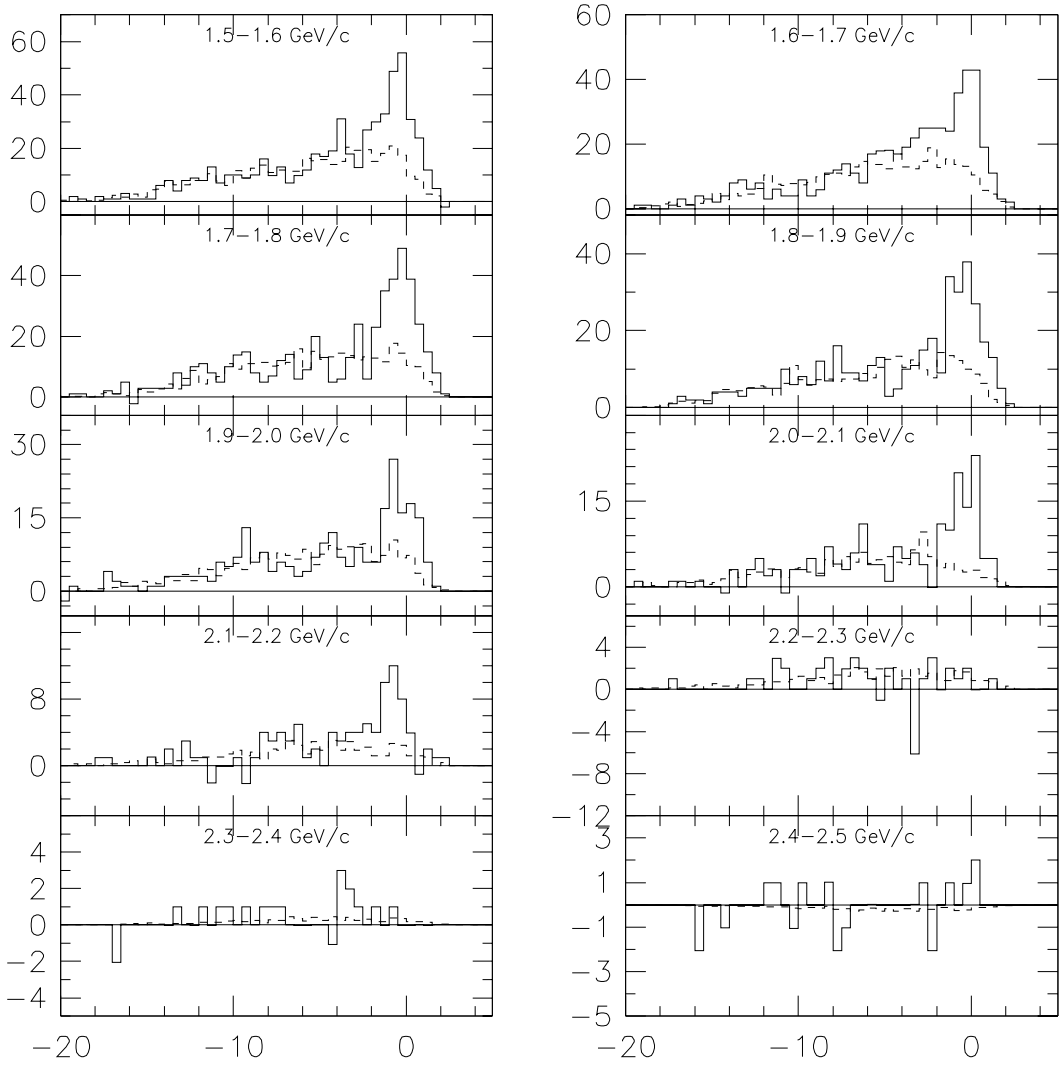

Figure 4.11: $\tilde{M}_\nu^2$ bin-by-bin for second lepton (electron) momentum between 1.5-2.5 GeV/c

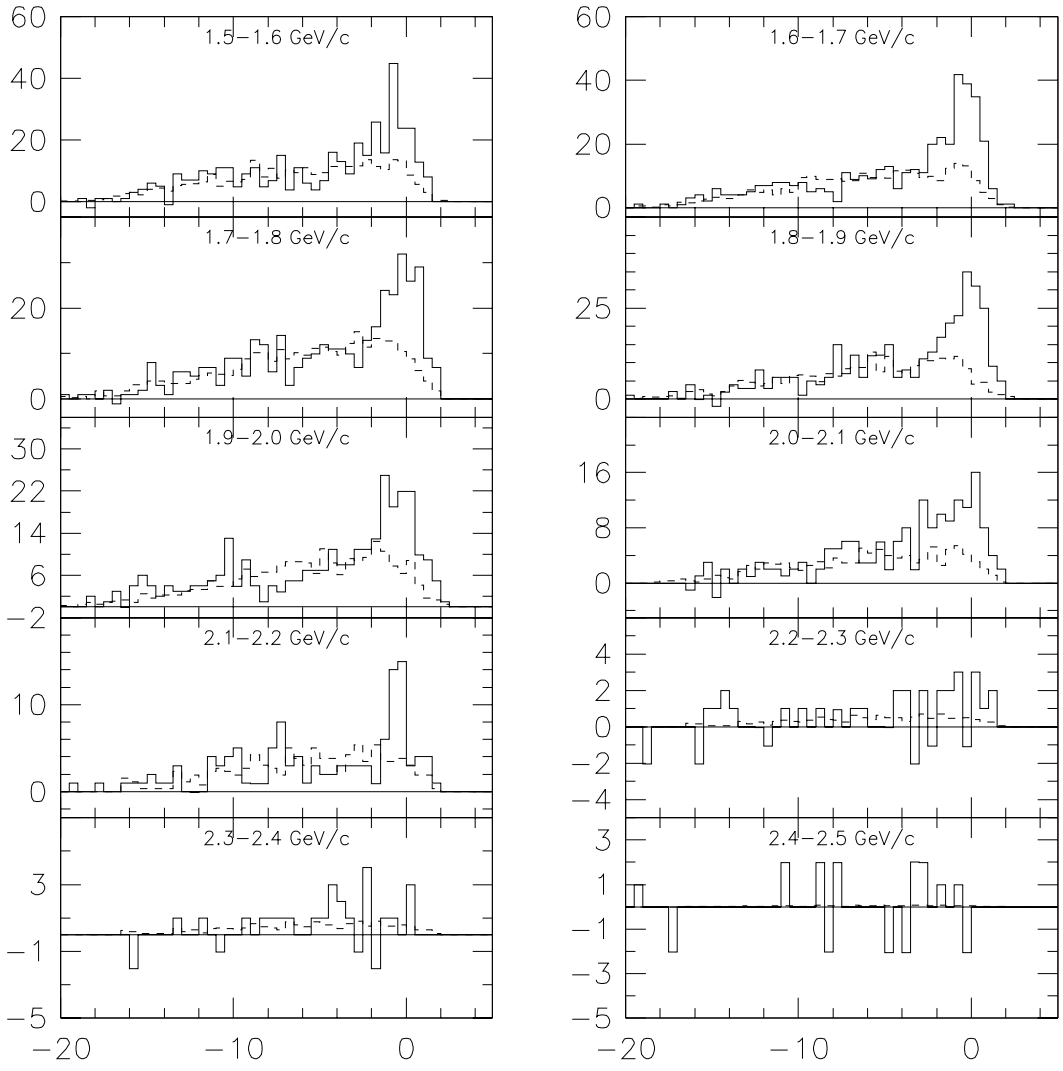

Figure 4.12: $\tilde{M}_\nu^2$ bin-by-bin for second lepton (muon) momentum between 1.5-2.5 GeV/c

Table 4.2: Second Lepton Spectrum

(GeV/c)	Data	MC	Data-MC	ϵ_{ID}	net event
electrons					
0.5-0.6	861.0 ± 33.5	340.2 ± 16.7	520.8 ± 37.5	0.548	950.7 ± 68.4
0.6-0.7	636.8 ± 29.1	228.8 ± 13.1	408.0 ± 31.9	0.582	700.9 ± 54.9
0.7-0.8	472.9 ± 23.6	176.0 ± 11.3	296.8 ± 26.2	0.585	507.1 ± 44.8
0.8-0.9	445.9 ± 23.3	146.1 ± 10.5	299.8 ± 25.6	0.593	505.2 ± 43.1
0.9-1.0	357.4 ± 20.1	119.3 ± 9.4	238.0 ± 22.1	0.598	398.0 ± 37.0
1.0-1.1	339.1 ± 20.3	110.6 ± 9.0	228.5 ± 22.2	0.615	371.4 ± 36.2
1.1-1.2	260.8 ± 17.2	90.7 ± 8.7	170.1 ± 19.3	0.621	274.0 ± 31.0
1.2-1.3	277.7 ± 17.3	105.7 ± 9.5	172.0 ± 19.7	0.622	276.5 ± 31.7
1.3-1.4	280.7 ± 17.4	102.7 ± 9.2	178.1 ± 19.6	0.618	288.0 ± 31.7
1.4-1.5	232.0 ± 16.3	95.6 ± 8.5	136.4 ± 18.4	0.625	218.2 ± 29.4
1.5-1.6	237.3 ± 16.2	94.8 ± 9.0	142.5 ± 18.5	0.635	224.4 ± 29.2
1.6-1.7	205.5 ± 15.0	77.8 ± 7.9	127.7 ± 16.9	0.635	200.9 ± 26.7
1.7-1.8	232.8 ± 15.3	84.2 ± 8.4	148.6 ± 17.4	0.636	233.8 ± 27.4
1.8-1.9	173.8 ± 13.4	68.8 ± 7.6	105.0 ± 15.4	0.638	164.6 ± 24.2
1.9-2.0	105.7 ± 10.9	43.8 ± 6.0	61.9 ± 12.4	0.635	97.5 ± 19.6
2.0-2.1	87.8 ± 10.0	20.2 ± 3.7	67.6 ± 10.7	0.637	106.1 ± 16.8
2.1-2.2	40.8 ± 7.3	8.4 ± 2.3	32.4 ± 7.7	0.648	50.1 ± 11.9
2.2-2.3	5.8 ± 4.3	1.6 ± 0.6	4.2 ± 4.4	0.630	6.7 ± 6.9
2.3-2.4	2.0 ± 1.4	0.2 ± 0.1	1.8 ± 1.4	0.619	2.9 ± 2.3
2.4-2.5	3.9 ± 3.2	0.0 ± 0.1	3.9 ± 3.2	0.615	6.3 ± 5.2
muons					
1.5-1.6	152.7 ± 13.7	65.5 ± 7.5	87.1 ± 15.6	0.409	212.9 ± 38.2
1.6-1.7	184.0 ± 14.8	63.5 ± 7.1	120.5 ± 16.4	0.463	259.9 ± 35.4
1.7-1.8	163.6 ± 14.1	69.3 ± 7.6	94.4 ± 16.0	0.483	195.5 ± 33.2
1.8-1.9	163.3 ± 13.6	54.2 ± 6.7	109.1 ± 15.2	0.503	217.0 ± 30.2
1.9-2.0	124.5 ± 11.8	53.1 ± 7.1	71.4 ± 13.8	0.513	139.1 ± 26.8
2.0-2.1	71.1 ± 8.9	22.8 ± 4.5	48.3 ± 9.9	0.528	91.5 ± 18.8
2.1-2.2	47.3 ± 7.4	17.9 ± 3.5	29.4 ± 8.2	0.540	54.3 ± 15.1
2.2-2.3	11.5 ± 5.0	0.6 ± 0.7	10.9 ± 5.0	0.529	20.6 ± 9.5
2.3-2.4	2.6 ± 3.1	0.3 ± 0.2	2.3 ± 3.1	0.540	4.2 ± 5.7
2.4-2.5	-0.2 ± 2.5	0.0 ± 0.0	-0.2 ± 2.5	0.536	-0.4 ± 4.7

4.8.2 Second Lepton Momentum Spectrum Correction

Lepton Efficiency Correction

This inclusive lepton momentum spectrum needs to be corrected for the detection efficiency. There are three factors affecting lepton detection: (1) general charged track finding, (2) lepton identification and (3) our geometrical cut in accepting the leptons.

The charged track finding efficiency is the charged track reconstruction efficiency. The lepton identification efficiency comes from the cut we made on lepton identification: $R2ELEC > 3$ for electrons, $MUQUAL = 0$ and $DPTHMU > 5$ for muon candidates. The geometrical acceptance was due to the fact that we accept electrons within region $cos\theta \leq 0.71$ and muons within $cos\theta \leq 0.61$ in our search for additional leptons within the tagged event. Except for this geometrical acceptance cut, the tracking and lepton identification cuts are a function of the momentum of the charged track.

The lepton identification and tracking reconstruction efficiency have been examined in detail by the previous CLEO analysis [46] as mentioned earlier. Since we use essentially the same lepton cuts as that analysis, we adopt that efficiency number and corrected for our geometrical acceptance cut. Our raw additional lepton momentum spectrum is then corrected by this efficiency bin-by-bin.

$B \to XJ/\psi \to \ell^+\ell^-$ Subtraction

To estimate the number of leptons from J/ψ decay, we use the generator level Monte Carlo to simulate the momentum spectrum of leptons from J/ψ and normalize to data. The normalization is found by pairing an identified muon with any oppositely charged track in the event to form the J/ψ invariant mass distribution for both data and Monte Carlo. This invariant mass distribution was fit with a Gaussian plus a smooth background curve.

The ratio of entries in the Gaussian in data to Monte Carlo is our scaling factor, which will multiply the Monte Carlo J/ψ lepton momentum spectrum to obtain the J/ψ lepton distribution in data.

It is estimated that we have 15.3 ± 3.2 (22.7 ± 4.4) for J/ψ electron (muon) in our reconstructed additional lepton momentum spectrum.

4.9 Extracting Primary Leptons

We use a phenomenological model to fit this corrected lepton spectrum to estimate the contributions from primary and secondary leptons. The result of the fit needs to be corrected for the tagging efficiency difference for events of tag with additional leptons and events with the tag alone.

4.9.1 Fitting

The resulting additional lepton spectrum is the combination of primary leptons, $b \to X\ell\bar{\nu}$, and secondary leptons, $b \to c \to X\ell\bar{\nu}$, from B meson decay. We have introduced in chapter 2 the theoretical functions for extracting the primary leptons. In this analysis, the central value was read out from the fit result of the ACCMM function because this function gives the best fit to the previous CLEO inclusive lepton spectrum analysis [46].

For fitting purposes, we put electrons and muons in a single plot by placing electrons at momentum 0-4 GeV/c and add 4 GeV/c to muons to place it at momentum 4-8 GeV/c. The purpose is to fit the electron and muon spectrum simultaneously, assuming lepton universality. This procedure has been employed by a previous CLEO analysis [46]. The result of the fit can be seen in Fig 4.13.

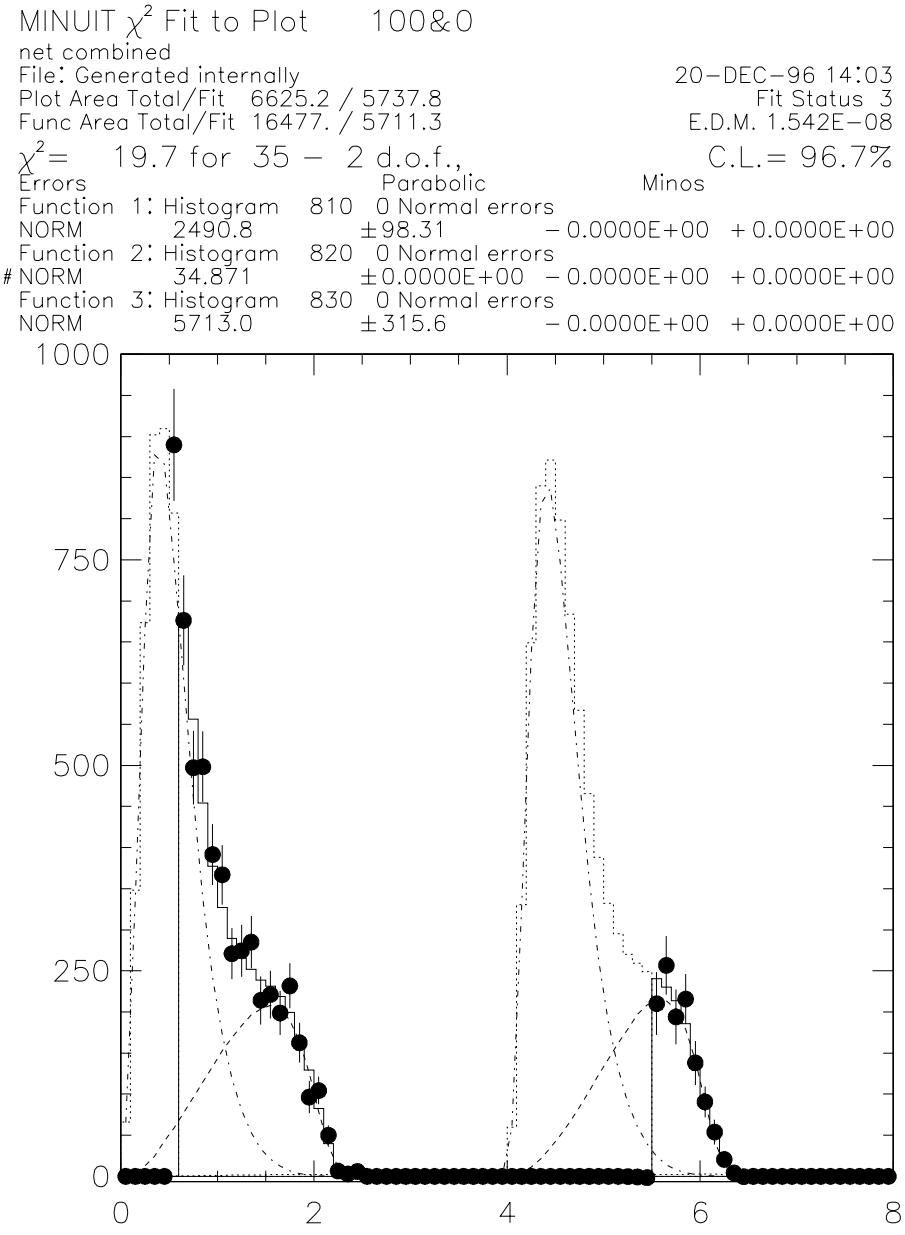

Figure 4.13: B decay lepton spectrum for simultaneous fit using ACCMM model. The electron is located from 0-4 GeV/c and muon is at 4-8 GeV/c.

4.9.2 Tagging Efficiency Correction

The number of primary leptons from the fit will further be corrected for the di-lepton opening angle cut $|cos\theta| < 0.99$, the cut on accepting events due to its charged multiplicity, and the different tagging efficiency between the tag and its additional lepton subsample.

The cut on the di-lepton opening angle is to prevent over-counting one lepton as two tracks. The correction for this di-lepton opening angle cut is purely geometrical in nature.

Since we accept events with at least five charged tracks, the difference in charge multiplicity between generic $B\bar{B}$ events and semileptonic events needs to be corrected. A previous CLEO analysis has found that the mean value of charge multiplicity for a tag with additional leptons is slightly lower than that for the tag along [48], due to the fact that charge multiplicity of a semileptonic B decay is lower than that for a generic B decay. This finding caused 0.5% under-efficiency for accepting semileptonic event over accepting the generic $B\bar{B}$ event.

The correction of the combination of these two cuts is found to be $(+1.1 \pm 1.1)\%$ [48].

The third correction we have to make is the difference between the tagging efficiency of the tag and its additional leptons subsample, resulting from the fact that it is easier to reconstruct a tag in a semileptonic decay event than in a generic hadronic event, where the number of charged tracks in the latter environment is higher.

We use Monte Carlo to study the tagging efficiency difference between events containing the generic B decay and a semileptonic decay. We first construct the tagging efficiency as a function of charge multiplicity in a generic $B\bar{B}$ event. Next, we obtain the charge multiplicity distribution for the semileptonic event. The charge multiplicity function for this semileptonic event subsample was sorted according to the lepton momentum in 100 MeV/c bins. We then multiplied the tagging efficiency function by the charge multiplicity distribution of

semileptonic event bin-by-bin to find out the tagging efficiency of the B semileptonic event subsample. We found that the tagging efficiency for semileptonic events is independent of its leptonic momentum, and the number is about 1.029 ± 0.013 over-efficient compared to generic $B\bar{B}$ event.

The net correction of the all sources in our $N_{tag,\ell}$ is $(-1.8 \pm 1.7)\%$.

From the fit, We obtain 2529 ± 102 primary leptons. We have 2484 ± 100 after the tagging efficiency correction and di-lepton opening angle correction. We denote the ratio of the number of the additional primary lepton to the number of the tag as $b_{tag} = N(tag, \ell_{add})/N(tag)$. We have:

$$\boxed{b_{tag} = \frac{2484.0 \pm 100.0}{22880.0 \pm 283.0} = 10.86 \pm 0.46}$$

4.10 Comparison of Two Inclusive Lepton Spectra

The tagged spectra of electrons and muons, Figure 4.13, after subtracting the secondary leptons, are then divided by the corresponding inclusive spectra from a previous CLEO single lepton analysis, Figure 4.1, [46], bin-by-bin in the momentum region between 1.5-2.4 GeV/c. If the two primary spectra have the same shape, then the resulting distribution in this momentum range should be flat. The ratio of the two spectra is denoted as R. If the spectra have the same shape, R is constant and $R = b_{tag}/b_{incl}$, where b_{tag} and b_{incl} are the semileptonic branching fractions measured in the tagged and total events samples, respectively. The distributions appear indeed to be flat. They are thus fitted to a constant function. The values of R as a function of electron and muon momentum are shown in Fig 4.14 and Fig 4.15 respectively. The result of a flat straight line fit gives $R = 1.013 \pm 0.061$ with $\chi^2/DOF = 7.5/8$ for electrons and $R = 1.036 \pm 0.071$ with $\chi^2/DOF = 3.1/8$ for muons.

The weighted error average is:

$$\boxed{R = 1.023 \pm 0.046}$$

We also obtain R by taking the ratio of the primary contributions to the spectra from the fits described above, and find excellent agreement.

The flat distribution of R indicates that the lepton spectrum for $\bar{B}^0$ and B^- semileptonic decay are very similar. And this value, along with the measurement from the single lepton method, can lead us to obtain the semileptonic branching fraction for $\bar{B}^0$ and B^-, respectively.

4.11 Systematic Error on R

Since the procedures for obtaining tagged and inclusive spectra have been made nearly identical, many of the systematic errors are highly correlated and cancel approximately in the ratio R. Among these are errors from lepton tracking and identification efficiencies, subtraction of the ψ contributions, fake rates, and spectral shapes for fitting to find the secondary contribution.

All the systematic errors are tabulated in Table 4.3. The overall systematic error on R is found to be 3.5%.

4.11.1 Primary Leptons

The principal source for the primary lepton shape is the ACCMM model [17]. As a check, we use the primary lepton shape from ISGW**, a sum of exclusive modes using a function derived from the ISGW model [18], fixing D^*/D ratio at 2.3 and adjusting the D^{**} portion

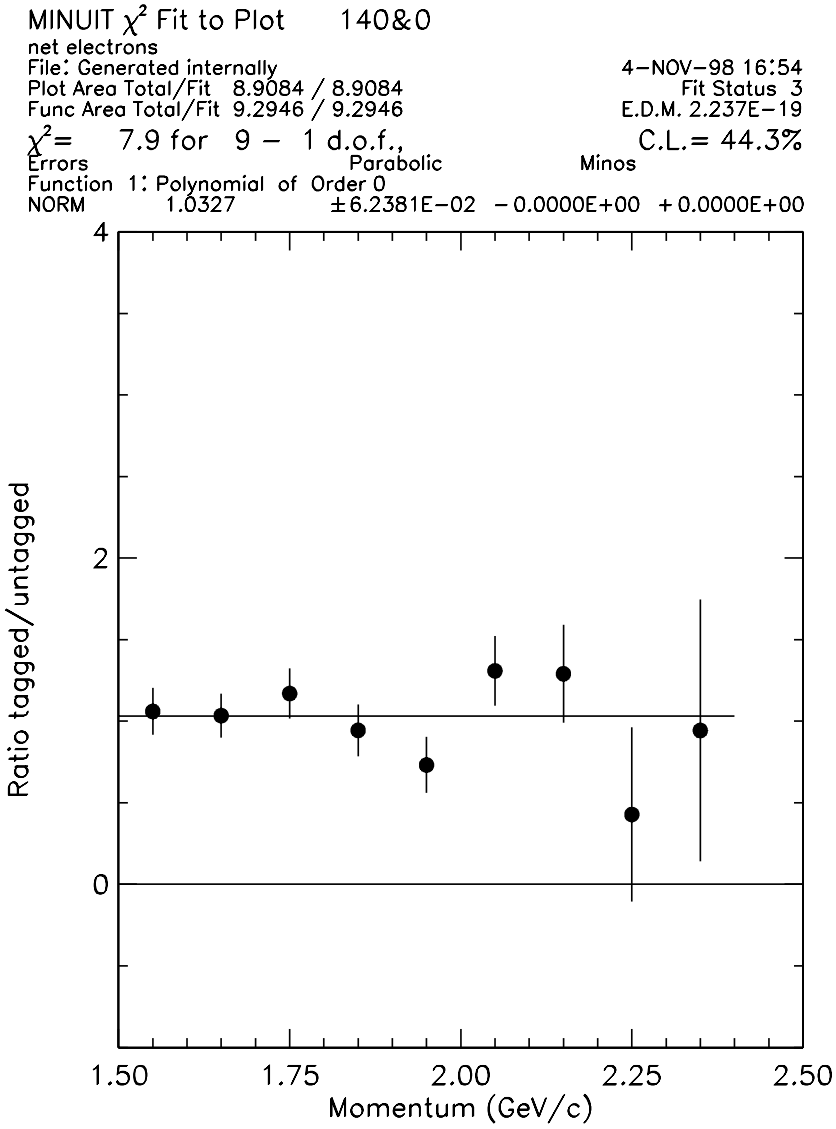

Figure 4.14: The lepton spectrum bin-by-bin comparison for single lepton inclusive measurement and this partial reconstruction method for electron momentum between 1.5-2.5 GeV/c

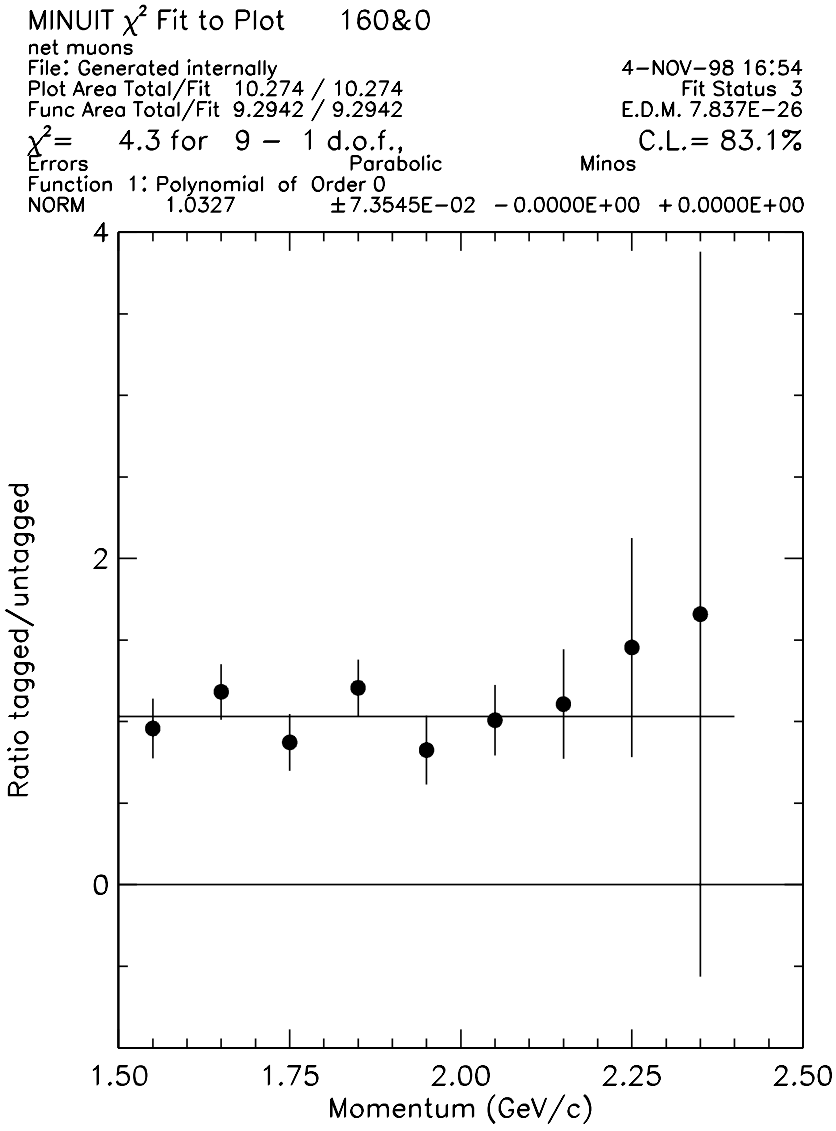

Figure 4.15: The lepton spectrum bin-by-bin comparison for single lepton inclusive measurement and this partial reconstruction method for muon momentum between 1.5-2.5 GeV/c

Table 4.3: Systematic Errors on R

Source	$\sigma_{sys}/value(\%)$	$\delta R/R$ (%)
Fake electron	50	0.1
Fake muon	25	0.2
$J\psi$ contribution	30	0.3
primary spectrum	isgw**[18]	0.3
secondary spectrum		2.3
Event/tag selection	1.7	1.7
Background estimate	1.0	1.0
$(b \to u)/(b \to c)$	21	–
other leptons	see text	1.7
$Total$		3.5%

to 21% to fit our tagged inclusive lepton spectrum, as shown in Fig 4.16. The choice of 21% D^{**}, as opposed to model prediction 11%, is based on the best fit result of previous CLEO analyses [48, 46]. We also shifted the primary lepton function up and down 50 MeV/c to check the result. To be conservative, we take the biggest deviation from the central value as our systematic error. It was found that the model uncertainty on primary leptons introduced 0.3% deviation from central value of R.

4.11.2 Secondary Leptons

We used the secondary lepton spectrum generated by the following procedure, as done by a previous CLEO analysis [78]. The lepton spectrum from the DELCO measurement [54] was boosted into the B meson lab frame to give the secondary lepton shape different from models to estimate the uncertainty of the secondary lepton spectrum in our fit. An analytic function was used by CLEO to refit the measured $D \to X\ell\nu$ leptonic spectrum [54]. The boost factor is obtained from the inclusive D momentum spectrum measured by CLEO-I.5 [77]. CLEO used a skewing function to multiply the D^0 and D^+ momentum spectrum to make the boosting harder or softer. The third change is that CLEO also varied the ratio of D^+ and D^0 up and down according to the measured D^+ and D^0 production ratio in B

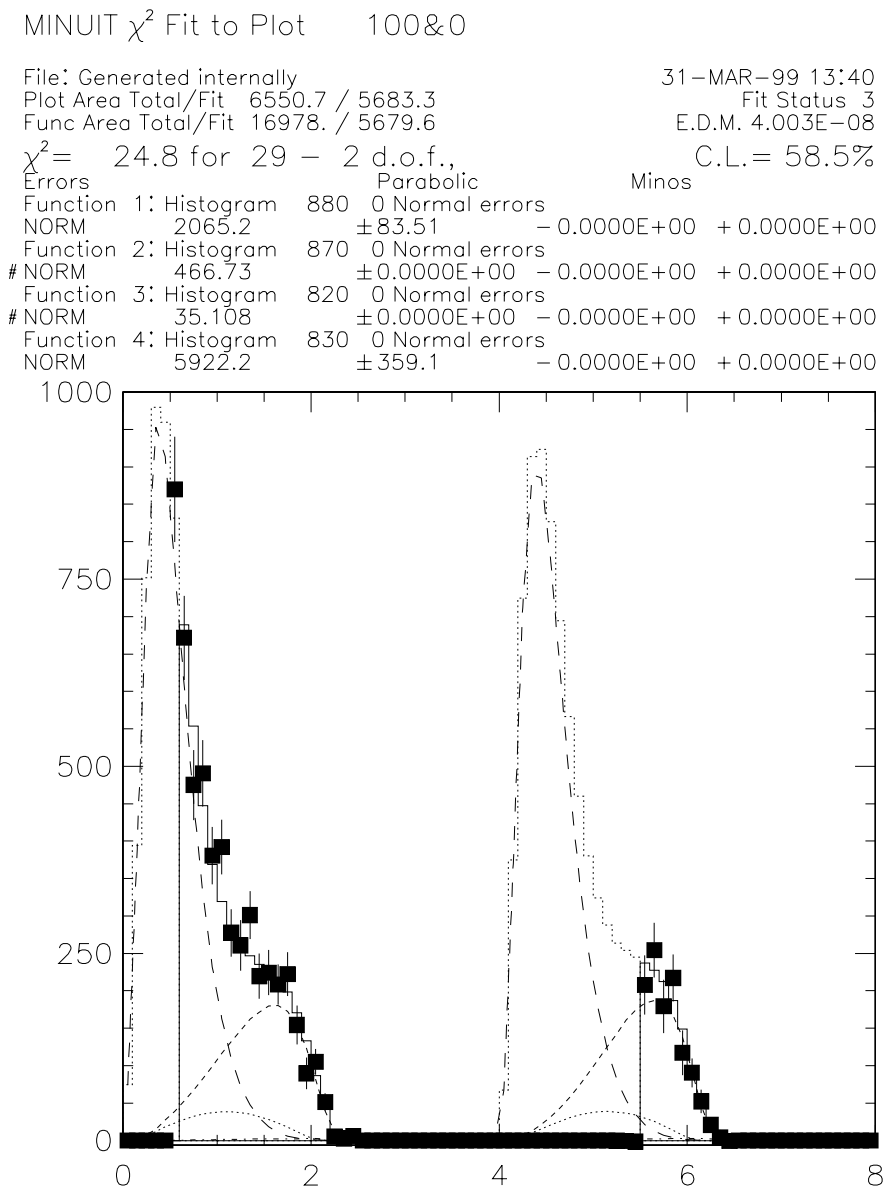

Figure 4.16: B decay lepton spectrum for simultaneous fit using ISGW** model. The electron is located from 0-4 GeV/c and muon is at 4-8 GeV/c.

decay [77]. We vary the uncertainties from the three sources up and down individually to get a series of secondary lepton spectra. We refit our lepton spectra by using those secondary shapes to evaluate the systematic error. We found the uncertainty of the secondary lepton spectrum introduces 2.3% systematic error in our value R.

4.11.3 Lepton from $B \to X\psi$ Decay

$B \to XJ/\psi, J/\psi \to \ell^+\ell^-$ introduces leptons from J/ψ in our additional lepton spectrum. Though this comprises a tiny portion of our additional lepton spectrum, we still need to study its efficiency carefully because it has a different spectrum shape from both the primary and secondary leptons.

The J/ψ lepton spectrum lies in the range $1.2 - 1.7$ GeV/c, where the primary leptons dominate. To understand the impact of this contribution, we varied the portion of leptons from J/ψ decay to see the result in our lepton spectrum fit. To be conservative, we moved it up and down by 30%, similarly to a previous CLEO inclusive lepton analysis [46]. This uncertainty contains the uncertainties of internal radiation of ψ and the contributions from ψ'. The result is found to be insensitive in our lepton spectra fit. We found the uncertainty on R to be 0.3%.

4.11.4 Fake Second Lepton

The effect of the fake lepton subtraction from our reconstructed inclusive lepton spectrum can be influential in our lepton spectrum fit. This subtraction can alter our additional lepton spectrum shape, thus changing the normalization for both primary and secondary leptons in the fit. We varied the electron and muon fake rate bin by bin up and down by 50% and 25% respectively to study the sensitivity. The uncertainty on fake rate comes from the difference

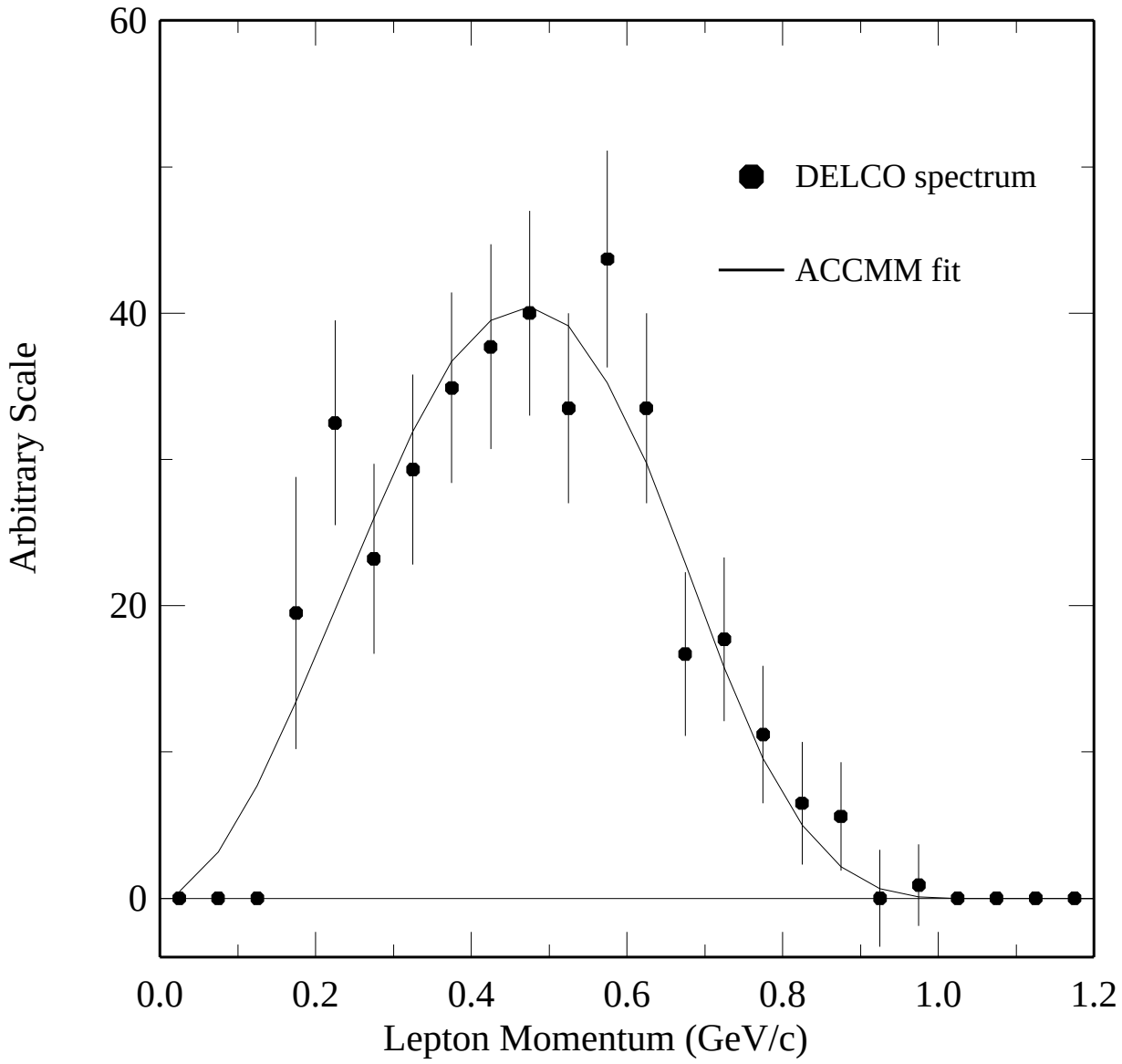

Figure 4.17: The ACCMM fit to DELCO Charm lepton spectrum

between the fake rate study of $\Upsilon(4S)$ and $\Upsilon(1S)$ [46].

We found the fit to our lepton spectra is insensitive to the uncertainties of the fake rate, which introduces a tiny 0.1% and 0.2% shift for fake electrons and muons respectively. This is not too surprising since the distribution of fake leptons above lepton momentum 1.5 GeV/c is very tiny, where the leptons from primary decay saturate the spectra and ultimately determine the normalization of the fit through our simultaneous fitting procedure.

4.11.5 Leptons from Other Sources

There are small numbers of leptons coming from sources other than primary, secondary and J/Ψ decay. Leptons could be from D_s, τ, Λ_c, π^0 Dalitz decay and from the process of converted photons. Our fit has approximated the spectra of all secondary leptons in the tagged spectra by those from D decay only. To estimate these uncertainty from these sources and from the fact that there may be small differences in shape between tagged and inclusive samples due to tag selection itself, we repeat the analysis after subtracting an estimated contributions of secondaries from sources other than D decay. We generate the spectrum shape of secondary leptons from sources other than D. We then combine this "other lepton" shape along with our primary and secondary lepton shape to fit our data. The portion that corresponds to "other lepton" as the result of the fit will then be subtracted from our lepton spectrum in the range 1.5-2.5 GeV/c. We vary it up and down according to the statistical fluctuation of the fit to estimate its systematic error on R. We found the shift to be 1.7% of R.

4.11.6 Systematic Error for Tag Only Events

There are uncertainties which apply only to the tagged but not to the inclusive measurement, including effects due to event selection, angular cuts and tagging efficiency differences. As was discussed in previous section, these contribute a total of 1.7%.

4.12 Spectrum Comparison Calculation

4.12.1 Estimation of Charged B Contamination

The N_{tag} has contributions not only from $\bar{B^0} \to D^{*+}\ell^-\bar{\nu_\ell}$, but also from $B \to D^{**}(D^*\pi)\ell\bar{\nu}$. Since D^{**} can decay to $D^*\pi$, the $\pi^\pm$ from D^* and the lepton can form a right sign tag pair with a missing mass square value near our signal region. Since both neutral and charged B can decay to $D^{**}/(D^*\pi)\ell\bar{\nu}$, we have $B^\pm$ contamination in our tag sample.

The charged B meson experiences D^{**} resonance decay:

$$B^- \to D^{**0}\ell^-\bar{\nu_\ell}, D^{**0} \to D^{*+}\pi^- \tag{4.9}$$

$$B^- \to D^{**0}\ell^-\bar{\nu_\ell}, D^{**0} \to D^{*0}\pi^0 \tag{4.10}$$

If we look at neutral B mesons experiencing similar D^{**} resonance decay, we have:

$$\bar{B^0} \to D^{**+}\ell^-\bar{\nu_\ell}, D^{**+} \to D^{*+}\pi^0 \tag{4.11}$$

$$\bar{B^0} \to D^{**+}\ell^-\bar{\nu_\ell}, D^{**+} \to D^{*0}\pi^+ \tag{4.12}$$

We can see that the $B \to D^{**}\ell\bar{\nu}$ components in our tag have sources from both charged and neutral B mesons. The composition of $B \to D^{**}\ell\bar{\nu}$ from charged and neutral B mesons is estimated by comparing the two decay widths. Using isospin symmetry, the ratio of the two decay widths becomes the production ratio of π^- to π^0 in $D^{**} \to D^*\pi$ decay. We obtain the ratio of charged to neutral B decay width in $B \to D^{**}\ell\bar{\nu}$ to be 2:1 based on this argument. A similar argument can be held for non-resonance decays, $B \to D^*\pi\ell\bar{\nu}_\ell$.

There was an exclusive analysis of $B \to D^{*+}\ell^-\bar{\nu}$ done with CLEO-I data [51]. That analysis calculated the M_ν^2 of the decay $B \to D^{*+}\ell^-\bar{\nu}$ where they reconstruct the D^0 and find the $D^* \to D^0\pi$ signal through the mass difference between D^* and D^0. They have estimated the contribution of $B \to D^{**+}/D^{*+}\pi\ell^-\bar{\nu}$ in the signal by combining the Monte Carlo shape of $B \to D^{**}/D^*\pi\ell\bar{\nu}$ with a Gaussian signal shape to fit their yield in the $\widetilde{M_\nu^2}$ signal region. They found the overall contributions from the resonant decay as well as the non-resonant decay in $B \to D^*\ell\bar{\nu}_\ell$ to comprise about 0.17 ± 0.10 times the contribution from $\bar{B}^0 \to D^{*+}\ell^-\bar{\nu}_\ell$. This makes our peak tag to have a fraction about 0.14 ± 0.08 coming from resonant or non-resonant decay [48]:

$$\boxed{f^{**} = 0.14 \pm 0.08}$$

We also use a measurement from ALEPH, $Br(B \to D^{*-}\pi^+\ell^+\nu X) = (1.25 \pm 0.16 \pm 0.12)\%$ [68], and a Monte Carlo simulation to obtain an independent value, $f^{**} = 0.10 \pm 0.02$, which is in agreement with the value measured by CLEO-I above. Here we use the CLEO-I value because it is more directly obtained, and our evaluation of b_0, b_+ and f_{00} are insensitive to it.

With $f^{**} = 0.14 \pm 0.08$, the charged B content in our tag peak area is then calculated as: $2\alpha f^{**}/(1 + 2\alpha) = (9.6 \pm 5.6)\%$ through the isospin symmetry argument we mentioned earlier. The α in the formula is defined as:

$$\alpha \equiv f_{+-}b_{+}/f_{00}b_{0} \tag{4.13}$$

where f_{+-} and f_{00} respectively correspond to the production fraction of charged and neutral B in $\Upsilon(4S)$ decay. b_+ and b_0 refer to the semileptonic branching fraction of charged and neutral B mesons respectively.

4.13 Calculation and Result

$$\begin{aligned}
b_{incl} &= f_{00}b_0 + f_{-+}b_+ = f_{00}b_0 \times (1 + \frac{f_{+-}b_+}{f_{00}b_0}) \\
&= f_{00}b_0(1+\alpha) \\
b_{tag} &= f_{0,tag}b_0 + f_{+,tag}b_+ \\
&= b_0(1 - f_{+,tag}) + f_{+,tag}\frac{b_+}{b_0} = b_0(1 + f_{+,tag}[\frac{b_+}{b_0} - 1]) = b_0(1 + f_{+,tag}[\beta - 1]) \\
&= b_0(1 + f_{+,tag}\delta\beta)
\end{aligned}$$

where $\alpha \equiv f_{+-}b_{+}/f_{00}b_{0}$, $\beta \equiv \frac{b_+}{b_0}$, $\delta\beta \equiv \beta - 1$, $f_{0,tag}$ and $f_{+,tag}$ correspond to the fraction of neutral and charged B candidates in our tag sample.

The calculation of b_0 and b_+ follows:

$$\begin{aligned}
b_0 &= \frac{b_{tag}}{1 + f_{+,tag}\delta\beta} = \frac{R \times b_{incl}}{1 + f_{+,tag}\delta\beta} \\
b_+ &= \beta b_0 = (\frac{R \times b_{incl}}{1 + f_{+,tag}\delta\beta})(1 + \delta\beta)
\end{aligned}$$

where $R \equiv b_{tag}/b_{incl}$

From the definition of R, we can obtain f_{00} as follows:

$$
\begin{aligned}
R &\equiv \frac{b_{tag}}{b_{incl}} = \frac{b_0(1+f_{+,tag}\delta\beta)}{f_{00}b_0(1+\alpha)} \\
\Rightarrow f_{00} &= \frac{1+f_{+,tag}\delta\beta}{R(1+\alpha)}
\end{aligned}
$$

From the definition of α and β, we can also get f_{00}:

$$
f_{00} = \frac{f_{+-}b_+}{\alpha b_0} = \frac{1+\delta\beta}{\alpha+1+\delta\beta} \tag{4.14}
$$

Thus we can obtain:

$$
(1+\delta R)(1+\alpha)(1+\delta\beta) = (1+f_{+,tag}\delta\beta)(1+\alpha+\delta\beta) \tag{4.15}
$$

Because $f_{+,tag}$, $\delta\beta$ and $\delta R \equiv R-1$ are expected to be small, (< 0.1), we can discard the term proportional to second order in $\delta\beta$, $f_{+,tag}(\delta\beta)^2$, to obtain a linear equation in $\delta\beta$:

$$
\delta\beta = \frac{\delta R(1+\alpha)}{(1+\alpha)(f_{+,tag}-\delta R)-\alpha} \tag{4.16}
$$

where $\delta\beta \equiv \beta - 1$,

There are two CLEO measurements for α value using isospin symmetry in B^- and B^0 decay:

$$
\alpha = \frac{Br(\Upsilon(4S)\to B^+B^-, B^-\to \bar{D^{*0}}\ell^+\bar{\nu}_\ell)}{Br(\Upsilon(4S)\to B^0\bar{B^0}, B^0\to \bar{D^{*-}}\ell^+\bar{\nu}_\ell)} = 1.14\pm0.14\pm0.13 \tag{4.17}
$$

see [52]

$$
\alpha = \frac{Br(\Upsilon(4S)\to B^+B^-, B^+\to \psi K^{(*)+})}{Br(\Upsilon(4S)\to B^0\bar{B^0}, B^0\to \psi K^{(*)+})} = 1.15\pm0.17\pm0.06 \tag{4.18}
$$

see [53]

The weighted error average of the two α value is 1.15±0.13. The $f_{+,tag}$ has been evaluated in previous section. Combining all these results together, we can calculate $\beta \equiv b_+/b_0$, and through α, we can calculate f_{+-}/f_{00}.

We can obtain $\beta = b_+/b_0$ through our measurements of $R = 1.023 \pm 0.046 \pm 0.036$, $f^{**} = 0.14 \pm 0.08$ and $\alpha = 1.15 \pm 0.13$:

$$\beta = 0.950^{+0.117+0.091}_{-0.080-0.068} \tag{4.19}$$

Since $\bar{B}^0$ and B^- form an isospin doublet, their semileptonic decay widths should be equal, so that β becomes the lifetime ratio of charged to neutral B mesons:

$$\begin{aligned} \frac{\tau_+}{\tau_0} &= \frac{\Gamma_{B^0}}{\Gamma_{B^-}} = \frac{\Gamma_{B^0}}{\Gamma_{B^0 \to X\ell\nu}} \times \frac{\Gamma_{B^- \to X\ell\nu}}{\Gamma_{B^-}} \\ &= \frac{b_+}{b_0} \end{aligned}$$

We can also calculate the fractional production of neutral to charged B mesons in $\Upsilon(4S)$ decay: f_{+-}/f_{00}. Based on the CLEO analysis of α and our measured b_+/b_0, we can calculate f_{+-}/f_{00} as follows:

$$\frac{f_{+-}}{f_{00}} = \frac{\alpha}{(\frac{b_+}{b_0})} \tag{4.20}$$

We obtain:

$$f_{+-}/f_{00} = 1.21 \pm 0.12 \pm 0.17 \tag{4.21}$$

We now can obtain the semileptonic branching fraction for neutral and charged B meson decay, $b_0 and b_+$, respectively, from our measured value for R and by using previous CLEO

measurement on averaged inclusive B semileptonic branching fraction, b_{incl}. By taking $b_{incl} = (10.49 \pm 0.46)\%$ [46], R and β as measured and calculated above, we obtain:

$$b_0 = (10.78 \pm 0.60 \pm 0.69)\% \tag{4.22}$$

$$b_+ = (10.25 \pm 0.57 \pm 0.65)\% \tag{4.23}$$